

Will Bilevel Optimizers Benefit from Loops

Kaiyi Ji*, Mingrui Liu†, Yingbin Liang‡ and Lei Ying§

June 1, 2022

Abstract

Bilevel optimization has arisen as a powerful tool for solving a variety of machine learning problems. Two current popular bilevel optimizers AID-BiO and ITD-BiO naturally involve solving one or two sub-problems, and consequently, whether we solve these problems with loops (that take many iterations) or without loops (that take only a few iterations) can significantly affect the overall computational efficiency. Existing studies in the literature cover only some of those implementation choices, and the complexity bounds available are not refined enough to enable rigorous comparison among different implementations. In this paper, we first establish unified convergence analysis for both AID-BiO and ITD-BiO that are applicable to all implementation choices of loops. We then specialize our results to characterize the computational complexity for all implementations, which enable an explicit comparison among them. Our result indicates that for AID-BiO, the loop for estimating the optimal point of the inner function is beneficial for overall efficiency, although it causes higher complexity for each update step, and the loop for approximating the outer-level Hessian-inverse-vector product reduces the gradient complexity. For ITD-BiO, the two loops always coexist, and our convergence upper and lower bounds show that such loops are necessary to guarantee a vanishing convergence error, whereas the no-loop scheme suffers from an unavoidable non-vanishing convergence error. Our numerical experiments further corroborate our theoretical results.

1 Introduction

Bilevel optimization has attracted significant attention recently due to its popularity in a variety of machine learning applications including meta-learning (Franceschi et al., 2018; Bertinetto et al., 2018; Rajeswaran et al., 2019; Ji et al., 2020a), hyperparameter optimization (Franceschi et al., 2018; Shaban et al., 2019; Feurer & Hutter, 2019), reinforcement learning (Konda & Tsitsiklis, 2000; Hong et al., 2020), and signal processing (Kunapuli et al., 2008; Flamary et al., 2014). In this paper, we consider the bilevel optimization problem that takes the following formulation.

$$\min_{x \in \mathbb{R}^p} \Phi(x) := f(x, y^*(x)) \quad \text{s.t.} \quad y^*(x) = \arg \min_{y \in \mathbb{R}^q} g(x, y), \quad (1)$$

where the outer- and inner-level functions f and g are both jointly continuously differentiable. We focus on the setting where the lower-level function g is strongly convex with respect to (w.r.t.) y with the condition number $\kappa = \frac{L}{\mu}$ (where L and μ are gradient Lipschitzness and strong convexity coefficients defined respectively

*Department of EECS, University of Michigan, Ann Arbor; e-mail: kaiyiji@umich.edu

†Department of CS, George Mason University; e-mail: mingruil@gmu.edu

‡Department of ECE, The Ohio State University; e-mail: liang.889@osu.edu

§Department of EECS, University of Michigan, Ann Arbor; e-mail: leiyiing@umich.edu

Table 1: Comparison of computational complexities of four AID-BiO implementations for finding an ϵ -accurate stationary point. For a fair comparison, gradient descent (GD) is used to solve the linear system for all algorithms. MV(ϵ): the total number of Jacobian- and Hessian-vector product computations. Gc(ϵ): the total number of gradient computations. $\tilde{\mathcal{O}}$: hide $\ln \frac{\kappa}{\epsilon}$ factors.

Algorithms	Q	N	MV(ϵ)	Gc(ϵ)
BA (Ghadimi & Wang, 2018)	$\Theta(\kappa \ln \kappa)$	$\frac{(k+1)^{\frac{1}{4}}}{2}$ (k : iteration number)	$\tilde{\mathcal{O}}(\kappa^5 \epsilon^{-1})$	$\tilde{\mathcal{O}}(\kappa^5 \epsilon^{-1.25})$
AID-BiO (Ji et al., 2021)	$\Theta(\kappa \ln \kappa)$	$\Theta(\kappa \ln \kappa)$	$\tilde{\mathcal{O}}(\kappa^4 \epsilon^{-1})$	$\tilde{\mathcal{O}}(\kappa^4 \epsilon^{-1})$
N - Q -loop AID (this paper)	$\Theta(\kappa \ln \kappa)$	$\Theta(\kappa \ln \kappa)$	$\tilde{\mathcal{O}}(\kappa^4 \epsilon^{-1})$	$\tilde{\mathcal{O}}(\kappa^4 \epsilon^{-1})$
Q -loop AID (this paper)	$\Theta(\kappa \ln \kappa)$	1	$\tilde{\mathcal{O}}(\kappa^6 \epsilon^{-1})$	$\tilde{\mathcal{O}}(\kappa^5 \epsilon^{-1})$
N -loop AID (this paper)	$\mathcal{O}(1)$	$\Theta(\kappa \ln \kappa)$	$\tilde{\mathcal{O}}(\kappa^4 \epsilon^{-1})$	$\tilde{\mathcal{O}}(\kappa^5 \epsilon^{-1})$
No-loop AID (this paper)	$\mathcal{O}(1)$	1	$\tilde{\mathcal{O}}(\kappa^6 \epsilon^{-1})$	$\tilde{\mathcal{O}}(\kappa^6 \epsilon^{-1})$

in Assumptions 1 and 3 in Section 3), and the outer-level objective function $\Phi(x)$ is possibly nonconvex w.r.t. x . Such types of geometries arise in many applications including meta-learning (which uses the last layer of neural networks as adaptation parameters), hyperparameter optimization (e.g., data hyper-cleaning and regularized logistic regression) and learning in communication networks (e.g., network utility maximization).

A variety of algorithms have been proposed to solve the bilevel optimization problem in eq. (1). For example, Hansen et al. (1992); Shi et al. (2005); Moore (2010) proposed constraint-based approaches by replacing the inner-level problem with its optimality conditions as constraints. In comparison, gradient-based bilevel algorithms have received intensive attention recently due to the effectiveness and simplicity, which include two popular approaches via approximate implicit differentiation (AID) (Domke, 2012; Pedregosa, 2016; Grazi et al., 2020; Ji et al., 2021) and iterative differentiation (ITD) (Maclaurin et al., 2015; Franceschi et al., 2017; Shaban et al., 2019). Readers can refer to Appendix A for an expanded list of related work.

Consider the AID-based bilevel approach (which we call AID-BiO). Its base iteration loop updates the variable x until convergence. Within such a base loop, it needs to solve two sub-problems: finding a nearly optimal solution of the inner-level function via N iterations, and approximating the outer-level Hessian-inverse-vector product via Q iterations. If Q and N are chosen to be large, then the corresponding iterations form **additional loops** of iterations within the base loop, which we respectively call as Q -loop and N -loop. Thus, AID-BiO can have four popular implementations depending on different choices of N and Q : N -loop (with large $N = \kappa \ln \kappa$ and small $Q = \mathcal{O}(1)$), N - Q -loop (with large $N = \Theta(\kappa \ln \kappa)$ and large $Q = \Theta(\kappa \ln \kappa)$), Q -loop (with $N = 1$ and $Q = \Theta(\kappa \ln \kappa)$), and No-loop (with $N = 1$ and $Q = \mathcal{O}(1)$). Note that No-loop refers to no additional loops within the base loop, and can be understood as conventional single-(base)-loop algorithms. These implementations can significantly affect the efficiency of AID-BiO. Generally, large Q (i.e., a Q -loop) provides a good approximation of the Hessian-inverse-vector product for the hypergradient computation, and large N (i.e., a N -loop) finds an accurate optimal point of the inner function. Hence, an algorithm with N -loop and Q -loop require fewer base-loop steps to converge, but each such base-loop step requires more computations due to these loops. On the other hand, small Q and/or N avoid computations of loops in each base-loop step, but can cause the algorithm to converge with many more base-loop steps. An intriguing question here is which implementation is overall most efficient and whether AID-BiO benefits from having N -loop and/or Q -loop. Existing theoretical studies on AID-BiO are far from answering this

Table 2: Comparison of computational complexities of two ITD-BiO implementations for finding an ϵ -accurate stationary point. For a fair comparison, gradient descent (GD) is used to solve the inner-level problem. The analysis in Ji et al. (2021) for ITD-BiO assumes that the inner-loop minimizer $y^*(x_k)$ is bounded at k^{th} iteration, which is not required in our analysis. μ : the strong-convexity constant of inner-level function $g(x, \cdot)$. For the last two columns, 'N/A' means that the complexities to achieve an ϵ -accuracy are not measurable due to the nonvanishing convergence error.

Algorithms	N	Convergence rate	$\mathbf{MV}(\epsilon)$	$\mathbf{Gc}(\epsilon)$
ITD-BiO (Ji et al., 2021)	$\Theta(\kappa \ln \kappa)$	$\mathcal{O}\left(\frac{\kappa^3}{K} + \epsilon\right)$	$\tilde{\mathcal{O}}(\kappa^4 \epsilon^{-1})$	$\tilde{\mathcal{O}}(\kappa^4 \epsilon^{-1})$
N - N -loop ITD (this paper)	$\Theta(\kappa \ln \kappa)$	$\mathcal{O}\left(\frac{\kappa^3}{K} + \epsilon\right)$	$\tilde{\mathcal{O}}(\kappa^4 \epsilon^{-1})$	$\tilde{\mathcal{O}}(\kappa^4 \epsilon^{-1})$
No-loop ITD (this paper)	$\Theta(1)$	$\mathcal{O}\left(\frac{\kappa^3}{K} + \kappa^3\right)$	N/A	N/A
Lower bound (this paper)	$\Theta(1)$	$\Omega(\kappa^2)$	N/A	N/A

question. The studies (Ghadimi & Wang, 2018; Ji et al., 2021) on deterministic AID-BiO focused only on the N - Q -loop scheme. A few studies analyzed the stochastic AID-BiO, such as Li et al. (2021) on No-loop, and Hong et al. (2020); Khanduri et al. (2021) on Q -loop. Those studies were not refined enough to capture the computational differences among different implementations, and further those studies collectively did not cover all the four implementations either.

- The first contribution of this paper lies in the development of a unified convergence theory for AID-BiO, which is applicable to all choices of N and Q . We further specialize our general theorems to provide the computational complexity for all of the above four implementations (as summarized in Table 1). Comparison among them suggests that AID-BiO does benefit from both N -loop and Q -loop. This is in contrast to minimax optimization (a special case of bilevel optimization), where it is shown in Lin et al. (2020); Zhang et al. (2020) that (No-loop) gradient descent ascent (GDA) with $N = 1$ often outperforms (N -loop) GDA with $N = \kappa \ln \kappa$ (here N denotes the number of ascent iterations for each descent iteration). To explain the reason, the gradient w.r.t. x in bilevel optimization involves additional second-order derivatives (that do not exist in minimax optimization), which are more sensitive to the accuracy of the optimal point of the inner function. Therefore, a large N finds such a more accurate solution, and is hence more beneficial for bilevel optimization than minimax optimization.

Differently from AID-BiO, the ITD-based bilevel approach (which we call as ITD-BiO) constructs the outer-level hypergradient estimation via backpropagation along the N -loop iteration path, and $Q = N$ always holds. Thus, ITD-BiO has only two implementation choices: N - N -loop (with large $N = \kappa \ln \kappa$) and No-loop (with small $N = \mathcal{O}(1)$). Here, N - N -loop and No-loop also refer to additional loops for solving sub-problems within the ITD-BiO's base loop of updating the variable x . The only convergence rate analysis on ITD-BiO was provided in Ji et al. (2021) but only for N - N -loop, which does not suggest how N - N -loop compares with No-loop. It is still an open question whether ITD-BiO benefits from N -loops.

- The second contribution of this paper lies in the development of a unified convergence theory for ITD-BiO, which is applicable to all values of N . We then specialize our general theorem to provide the computational complexity for both of the above implementations (as summarized in Table 2). We further develop a convergence lower bound, which suggests that N - N -loop is necessary to guarantee

Algorithm 1 AID-based bilevel optimization (AID-BiO) with double warm starts

```
1: Input: Stepsizes  $\alpha, \beta > 0$ , initializations  $x_0, y_0, v_0$ .
2: for  $k = 0, 1, 2, \dots, K$  do
3:   Set  $y_k^0 = y_{k-1}^N$  if  $k > 0$  and  $y_0$  otherwise (warm start initialization)
4:   for  $t = 1, \dots, N$  do
5:     Update  $y_k^t = y_k^{t-1} - \alpha \nabla_y g(x_k, y_k^{t-1})$ 
6:   end for
7:   Hypergradient estimation via:
      Set  $v_k^0 = v_{k-1}^Q$  if  $k > 0$  and  $v_0$  otherwise (warm start initialization).
      Solve  $v_k^Q$  from  $\nabla_y^2 g(x_k, y_k^N) v = \nabla_y f(x_k, y_k^N)$  via  $Q$  steps of iterative algorithms starting from  $v_k^0$ 
      Compute  $\widehat{\nabla} \Phi(x_k) = \nabla_x f(x_k, y_k^N) - \nabla_x \nabla_y g(x_k, y_k^N) v_k^Q$ 
8:   Update  $x_{k+1} = x_k - \beta \widehat{\nabla} \Phi(x_k)$ 
9: end for
```

a vanishing convergence error, whereas the no-loop scheme suffers from an unavoidable non-vanishing convergence error.

The technical contribution of this paper is two-fold. For AID methods, most existing studies including Ji et al. (2021) solve the linear system with large $Q = \Theta(\kappa \log \kappa)$ so that the upper-level Hessian-inverse-vector product approximation error can vanish. In contrast, we allow arbitrary (possibly small) Q , and hence this upper-level error can be large and nondecreasing, posing a key challenge to guarantee convergence. We come up with a novel idea to prove the convergence by showing that this error, not by itself but jointly with the inner-loop error, admits an (approximately) iteratively decreasing property, which bounds the hypergradient error and yields convergence. The analysis contains new developments to handle the coupling between this error and the inner-loop error, which is critical in our proof. For ITD methods, unlike existing studies including Ji et al. (2021), we remove the boundedness assumption on $y^*(x)$ via a novel error analysis over the entire execution rather than a single iteration. Our analysis tools are general and can be extended to stochastic and acceleration bilevel optimizers.

2 Algorithms

2.1 AID-based Bilevel Optimization Algorithm

As shown in Algorithm 1, we present the general AID-based bilevel optimizer (which we refer to AID-BiO for short). At each iteration k of the base loop, AID-BiO first executes N steps of gradient decent (GD) over the inner function $g(x, y)$ to find an approximation point y_k^N , where N can be chosen either at a constant level or as large as $N = \kappa \ln \kappa$ (which forms an N -**loop** of iterations). Moreover, to accelerate the practical training and achieve a stronger performance guarantee, AID-BiO often adopts a warm-start strategy by setting the initialization y_k^0 of each N -loop to be the output y_{k-1}^N of the preceding N -loop rather than a random start.

To update the outer variable, AID-BiO adopts the gradient descent, by approximating the true gradient $\nabla \Phi(x_k)$ of the outer function w.r.t. x (called hypergradient) that takes the following form:

$$(\text{True hypergradient:}) \quad \nabla \Phi(x_k) = \nabla_x f(x_k, y^*(x_k)) - \nabla_x \nabla_y g(x_k, y^*(x_k)) v_k^*, \quad (2)$$

where v_k^* is the solution of the linear system $\nabla_y^2 g(x_k, y^*(x_k)) v = \nabla_y f(x_k, y^*(x_k))$. To approximate the above true hypergradient, AID-BiO first solves v_k^Q as an approximate solution to a linear system $\nabla_y^2 g(x_k, y_k^N) v =$

$\nabla_y f(x_k, y_k^N)$ using Q steps of GD iterations starting from v_k^0 . Here, Q can also be chosen either at a constant level or as large as $Q = \kappa \ln \frac{\kappa}{\mu}$ (which forms a **Q -loop** of iterations). Note that a warm start is also adopted here by setting $v_k^0 = v_{k-1}^Q$, which is critical to achieve the convergence guarantee for small Q . If Q is large enough, e.g., at an order of $\kappa \ln \frac{\kappa}{\mu}$, a zero initialization with $v_k^0 = 0$ suffices to solve the linear system well. Then, AID-BiO constructs a hypergradient estimator $\hat{\nabla}\Phi(x_k)$ given by

$$(\text{AID-based hypergradient estimate:}) \quad \hat{\nabla}\Phi(x_k) = \nabla_x f(x_k, y_k^N) - \nabla_x \nabla_y g(x_k, y_k^N) v_k^Q. \quad (3)$$

Note that the execution of AID-BiO involves only Hessian-vector products in solving the linear system and Jacobian-vector product $\nabla_x \nabla_y g(x_k, y_k^N) v_k^Q$ which are more computationally tractable than the calculation of second-order derivatives.

It is clear that different choices of N and Q lead to four implementations within the base loop of AID-BiO: N -loop (with large $N = \kappa \ln \kappa$ and small $Q = \mathcal{O}(1)$), N - Q -loop (with large $N = \kappa \ln \kappa$ and $Q = \kappa \ln \kappa$), Q -loop (with small $N = 1$ and large $Q = \kappa \ln \kappa$) and No-loop (with small $N = 1$ and $Q = \mathcal{O}(1)$). In Section 4, we will establish a unified convergence theory for AID-BiO applicable to all its implementations in order to formally compare their computational efficiency.

2.2 ITD-Based Bilevel Optimization Algorithm

As shown in Algorithm 2, the ITD-based bilevel optimizer (which we refer to as ITD-BiO) updates the inner variable y similarly to AID-BiO, and obtains the N -step output y_k^N of GD with a warm-start initialization. ITD-BiO differentiates from AID-BiO mainly in its estimation of the hypergradient. Without leveraging the implicit gradient formulation, ITD-BiO computes a direct derivative $\frac{\partial f(x_k, y_k^N)}{\partial x_k}$ via automatic differentiation for hypergradient approximation. Since y_k^N has a dependence on x_k through the N -loop iterative GD updates, the execution of ITD-BiO takes the backpropagation over the entire N -loop trajectory. To elaborate, it can be shown via the chain rule that the hypergradient estimate $\frac{\partial f(x_k, y_k^N)}{\partial x_k}$ takes the following form of $\frac{\partial f(x_k, y_k^N)}{\partial x_k} = \nabla_x f(x_k, y_k^N) - \alpha \sum_{t=0}^{N-1} \nabla_x \nabla_y g(x_k, y_k^t) \prod_{j=t+1}^{N-1} (I - \alpha \nabla_y^2 g(x_k, y_k^j)) \nabla_y f(x_k, y_k^N)$. As shown in this equation, the differentiation does not compute the second-order derivatives directly but compute more tractable and economical Hessian-vector products $\nabla_y^2 g(x_k, y_k^{j-1}) v_j, j = 1, \dots, N$ (similarly for Jacobian-vector products), where each v_j is obtained recursively via $v_{j-1} = (I - \alpha \nabla_y^2 g(x_m, y_m^j)) v_j$ with $v_N = \nabla_y f(x_m, y_m^N)$.

Clearly, the implementation of ITD-BiO implies that $N = Q$ always holds. Hence, ITD-BiO takes only two possible architectures within its base loop: N - N -loop (with large $N = \kappa \ln \frac{\kappa}{\epsilon}$) and No-loop (with small $N = 1$). In Section 5, we will establish a unified convergence theory for ITD-BiO applicable to both of its implementations in order to formally compare their computational efficiency.

3 Definitions and Assumptions

This paper focuses on the following types of objective functions.

Assumption 1. *The inner-level function $g(x, y)$ is μ -strongly-convex w.r.t. y .*

Since the objective function $\Phi(x)$ in eq. (1) is possibly nonconvex, algorithms are expected to find an ϵ -accurate stationary point defined as follows.

Definition 1. *We say \bar{x} is an ϵ -accurate stationary point for the bilevel optimization problem given in eq. (1) if $\|\nabla\Phi(\bar{x})\|^2 \leq \epsilon$, where \bar{x} is the output of an algorithm.*

Algorithm 2 ITD-based bilevel optimization algorithm (ITD-BiO) with warm start

```
1: Input: Stepsize  $\alpha > 0$ , initializations  $x_0$  and  $y_0$  .
2: for  $k = 0, 1, 2, \dots, K$  do
3:   Set  $y_k^0 = y_{k-1}^N$  if  $k > 0$  and  $y_0$  otherwise (warm start initialization)
4:   for  $t = 1, \dots, N$  do
5:     Update  $y_k^t = y_k^{t-1} - \alpha \nabla_y g(x_k, y_k^{t-1})$ 
6:   end for
7:   Compute  $\widehat{\nabla} \Phi(x_k) = \frac{\partial f(x_k, y_k^N)}{\partial x_k}$  via backpropagation w.r.t.  $x_k$ 
8:   Update  $x_{k+1} = x_k - \beta \widehat{\nabla} \Phi(x_k)$ 
9: end for
```

In order to compare the performance of different bilevel algorithms, we adopt the following metrics of computational complexity.

Definition 2. Let $Gc(\epsilon)$ be the number of gradient evaluations, and $MV(\epsilon)$ be the total number of Jacobian- and Hessian-vector product evaluations to achieve an ϵ -accurate stationary point of the bilevel optimization problem in eq. (1).

Let $z = (x, y)$. We take the following standard assumptions, as also widely adopted by Ghadimi & Wang (2018); Ji et al. (2020a).

Assumption 2. Gradients $\nabla f(z)$ and $\nabla g(z)$ are L -Lipschitz, i.e., for any z, z' ,

$$\|\nabla f(z) - \nabla f(z')\| \leq L\|z - z'\|, \quad \|\nabla g(z) - \nabla g(z')\| \leq L\|z - z'\|.$$

As shown in eq. (2), the gradient of the objective function $\Phi(x)$ involves the second-order derivatives $\nabla_x \nabla_y g(z)$ and $\nabla_y^2 g(z)$. The following assumption imposes the Lipschitz conditions on such higher-order derivatives, as also made in Ghadimi & Wang (2018).

Assumption 3. Suppose the derivatives $\nabla_x \nabla_y g(z)$ and $\nabla_y^2 g(z)$ are ρ -Lipschitz, i.e., for any z, z'

$$\|\nabla_x \nabla_y g(z) - \nabla_x \nabla_y g(z')\| \leq \rho\|z - z'\|, \quad \|\nabla_y^2 g(z) - \nabla_y^2 g(z')\| \leq \rho\|z - z'\|.$$

To guarantee the boundedness the hypergradient estimation error, existing works (Ghadimi & Wang, 2018; Ji et al., 2020a; Grazi et al., 2020) assume that the gradient $\nabla f(z)$ is bounded for all $z = (x, y)$. Instead, we make a weaker boundedness assumption on the gradients $\nabla_y f(x, y^*(x))$.

Assumption 4. There exists a constant M such that for any x , $\|\nabla_y f(x, y^*(x))\| \leq M$.

For the case where the total objective function $\Phi(\cdot)$ has some benign structures, e.g., convexity or strong convexity, Assumption 4 can be removed by an induction analysis that all iterates are bounded as in Ji & Liang (2021). Assumption 4 can also be removed by projecting x onto a bounded constraint set \mathcal{X} .

4 Convergence Analysis of AID-BiO

As we describe in Section 2.1, AID-BiO can have four possible implementations depending on whether N and Q are chosen to be large enough to form an N -loop and/or Q -loop. In this section, we will provide the convergence analysis and characterize the overall computational complexity for all of the four implementations, which will provide the general guidance on which algorithmic architecture is computationally most efficient.

4.1 Convergence Rate and Computational Complexity

In this subsection, we develop two unified theorems for AID-BiO, both of which are applicable to all the regimes of N and Q . We then specialize these theorems to provide the complexity bounds (as corollaries) for the four implementations of AID-BiO. It turns out that the first theorem provides tighter complexity bounds for the implementations with small $Q = \Theta(1)$, and the second theorem provides tighter complexity bounds for the implementations with large $Q = \kappa \ln \frac{\kappa}{\epsilon}$. Our presentation of those corollaries below will thus focus only on the tighter bounds. The following theorem provides our first unified convergence analysis for AID-BiO.

Theorem 1. *Suppose Assumptions 1, 2, 3 and 4 hold. Choose parameters α, η and λ such that $(1 + \lambda)(1 - \alpha\mu)^N(1 + 4r(1 + \frac{1}{\eta\mu})L^2) \leq 1 - \eta\mu$, where $r = \frac{C_Q^2}{(\frac{\rho^2 M^2}{\mu} + L)^2}$ with $C_Q = \frac{Q(1-\eta\mu)^{Q-1}\rho M\eta}{\mu} + \frac{1-(1-\eta\mu)^Q(1+\eta Q\mu)}{\mu^2}\rho M + (1 - (1 - \eta\mu)^Q)\frac{L}{\mu}$. Let $L_\Phi = L + \frac{2L^2 + \rho M^2}{\mu} + \frac{2\rho LM + L^3}{\mu^2} + \frac{\rho L^2 M}{\mu^3}$ be the smoothness parameter of $\Phi(\cdot)$. Let $\tilde{w} := \frac{(1-\eta\mu)\eta\mu}{3\lambda r L^2}(1 + \frac{\rho^2 M^2}{L^2 \mu^2})\frac{L^2}{\mu^2} + (1 + \frac{1}{\eta\mu})(L^2 + \frac{\rho^2 M^2}{\mu^2})(\frac{16(1-\eta\mu)^{2Q}}{\mu^2} + \frac{4(1-\eta\mu)\eta\mu}{3\lambda L^2})\frac{L^2}{\mu^2}$. Choose the outer stepsize β such that $\beta = \min\{\frac{1}{12L_\Phi}, \sqrt{\frac{\eta\mu}{18L^2\tilde{w}}}\}$. Then,*

$$\frac{1}{K} \sum_{k=0}^{K-1} \|\nabla\Phi(x_k)\|^2 \leq \frac{8(\Phi(x_0) - \Phi(x^*))}{\beta K} + \frac{21L^2((1 + \frac{\rho^2 M^2}{L^2 \mu^2})\|y_0^*\|^2 + (\frac{3M}{\mu} + \frac{2L}{\mu}\|y_0^*\|)^2)}{\eta\mu K}. \quad (4)$$

Theorem 1 also elaborates the precise requirements on the stepsizes α, η and β and the auxiliary parameter λ , which take complicated forms. In the following, by further specifying these parameters, we characterize the complexities for AID-BiO in more explicit forms. We focus on the implementations with $Q = \Theta(1)$ (for which Theorem 1 specializes to tighter bound than Theorem 2 below), which includes the N -loop scheme (with $N = \Theta(\kappa \ln \kappa)$) and the No-loop scheme (with $N = 1$).

Corollary 1 (N -loop). *Consider N -loop AID-BiO with $N = \Theta(\kappa \ln \kappa)$ and $Q = \Theta(1)$, where $\kappa = \frac{L}{\mu}$ denotes the condition number of the inner problem. Under the same setting of Theorem 1, choose $\eta = \frac{1}{L}$, $\alpha = \frac{1}{L}$, and $\lambda = 1$. Then, we have $\frac{1}{K} \sum_{k=0}^{K-1} \|\nabla\Phi(x_k)\|^2 = \mathcal{O}(\frac{\kappa^4}{K} + \frac{\kappa^3}{K})$, and the complexity to achieve an ϵ -accurate stationary point is $\text{Gc}(\epsilon) = \tilde{\mathcal{O}}(\kappa^5 \epsilon^{-1})$, $\text{MV}(\epsilon) = \tilde{\mathcal{O}}(\kappa^4 \epsilon^{-1})$.*

Corollary 2 (No-loop). *Consider No-loop AID-BiO with $N = 1$ and $Q = \Theta(1)$. Under the same setting of Theorem 1, choose parameters $\alpha = \frac{1}{L}$, $\lambda = \frac{\alpha\mu}{2}$ and $\eta = \min\{\frac{1}{128} \frac{\alpha\mu^2}{Q^2 L^2}, \frac{\alpha}{4}, \frac{1}{\mu Q}\}$. Then, $\frac{1}{K} \sum_{k=0}^{K-1} \|\nabla\Phi(x_k)\|^2 = \mathcal{O}(\frac{\kappa^6}{K} + \frac{\kappa^5}{K})$, and the complexity is $\text{Gc}(\epsilon) = \tilde{\mathcal{O}}(\kappa^6 \epsilon^{-1})$, $\text{MV}(\epsilon) = \tilde{\mathcal{O}}(\kappa^6 \epsilon^{-1})$.*

The analysis of Theorem 1 can be further improved for the large Q regime, which guarantees a sufficiently small outer-level approximation error, and helps to relax the requirement on the stepsize η . Such an adaptation yields the following alternative unified convergence characterization for AID-BiO, which is applicable for all Q and N , but specializes to tighter complexity bounds than Theorem 1 in the large Q regime. For simplicity, we set the initialization $v_k^0 = 0$ in Algorithm 1.

Theorem 2. *Suppose Assumptions 1, 2, 3 and 4 hold. Define $\tau = (1 - \alpha\mu)^N(1 + \lambda + 6(1 + \lambda^{-1})(L^2 + \rho^2 M^2 \mu^{-2} + 2L^2 C_Q^2)L^2 \beta^2 \mu^{-2})$, $w = 6(1 - \alpha\mu)^N(L^2 + \rho^2 M^2 \mu^{-2} + 2L^2 C_Q^2)(1 + \lambda^{-1})L^2 \mu^{-2}$, where C_Q is a positive constant defined as in Theorem 1. Choose parameters α, β such that $\tau < 1$ and $\beta L_\Phi + w\beta^2(\frac{1}{2} + \beta L_\Phi)\frac{1}{1-\tau} \leq \frac{1}{4}$ hold. Then, the output of AID-BiO satisfies*

$$\frac{1}{K} \sum_{k=0}^{K-1} \|\nabla\Phi(x_k)\|^2 \leq \frac{4(\Phi(x_0) - \Phi(x^*))}{\beta K} + \frac{3}{K} \frac{\delta_0}{1 - \tau} + \frac{27L^2 M^2}{\mu^2} (1 - \eta\mu)^{2Q},$$

where $\delta_0 = 3(L^2 + \frac{\rho^2 M^2}{\mu^2} + 2L^2 C_Q^2)(1 - \alpha\mu)^N \|y_0^* - y_0\|^2$ is the initial distance.

We next specialize Theorem 2 to obtain the complexity for two implementations of AID-BiO with $Q = \Theta(\kappa \ln \kappa)$: N - Q -loop (with $N = \Theta(\kappa \ln \kappa)$) and Q -loop (with $N = 1$), as shown in the following two corollaries. For each case, we need to set the parameters λ, η and α in Theorem 2 properly.

Corollary 3 (N - Q -loop). *Consider N - Q -loop AID-BiO with $N = \Theta(\kappa \ln \kappa)$ and $Q = \Theta(\kappa \ln \frac{\kappa}{\epsilon})$. Under the same setting of Theorem 2, choose $\eta = \alpha = \frac{1}{L}$, $\lambda = 1$ and $\beta = \Theta(\kappa^{-3})$. Then, $\frac{1}{K} \sum_{k=0}^{K-1} \|\nabla \Phi(x_k)\|^2 = \mathcal{O}(\frac{\kappa^3}{K} + \epsilon)$, and the complexity is $\text{Gc}(\epsilon) = \tilde{\mathcal{O}}(\kappa^4 \epsilon^{-1})$, $\text{MV}(\epsilon) = \tilde{\mathcal{O}}(\kappa^4 \epsilon^{-1})$.*

Corollary 4 (Q -loop). *Consider Q -loop AID-BiO with $N = 1$ and $Q = \Theta(\kappa \ln \frac{\kappa}{\epsilon})$. Under the same setting of Theorem 2, choose $\alpha = \eta = \frac{1}{L}$, $\lambda = \frac{\alpha \mu}{2}$ and $\beta = \Theta(\kappa^{-4})$. Then, $\frac{1}{K} \sum_{k=0}^{K-1} \|\nabla \Phi(x_k)\|^2 = \mathcal{O}(\frac{\kappa^5}{K} + \frac{\kappa^4}{K} + \epsilon)$, and the complexity is $\text{Gc}(\epsilon) = \tilde{\mathcal{O}}(\kappa^5 \epsilon^{-1})$, $\text{MV}(\epsilon) = \tilde{\mathcal{O}}(\kappa^6 \epsilon^{-1})$.*

Discussion on hyperparameter selection for different implementations. For all loop-sizes, we set the hyperparameters to achieve the best complexity as long as convergence is guaranteed. Let us elaborate on N -loop (Corollary 1) and No-loop (Corollary 2). **At a proof level**, λ needs to satisfy $(1 - \alpha\mu)^N(1 + \lambda) < 1$ (see Lemma 2) to guarantee the convergence; otherwise the inner-loop error will explode. Given this requirement, for N -loop with $N = \Theta(\kappa \log \kappa)$, $\lambda = \Theta(1)$ achieves the best complexity. However, for No-loop with $N = 1$, the requirement becomes $(1 - \alpha\mu)(1 + \lambda) < 1$, and $\lambda = \Theta(\mu)$ achieves the best complexity. The stepsize η appears in $(1 - \alpha\mu)^N \frac{\eta}{\mu} \|y_{k-1}^N - y_{k-1}^*\|^2$ (see Lemma 1) of the error $\|v_k^Q - v_k^*\|^2$. Given the requirement $(1 - \alpha\mu)^N \frac{\eta}{\mu} < 1$, for N -loop with $N = \Theta(\kappa \log \kappa)$, $\eta = \Theta(1)$ achieves the best complexity, whereas for No-loop with $N = 1$, the best $\eta = \Theta(\mu)$. **At a conceptual level**, estimating the hypergradient and linear system contains the inner-loop error $\|y_k^N - y_k^*\|^2$. For $N = 1$, the per-iteration error is large, and hence we need smaller stepsizes λ, η, β to ensure the accumulated error not to explode. A similar argument holds for N - Q -loop and Q -loop.

4.2 Comparison among Four Implementations

Impact of N -loop ($N = 1$ vs $N = \kappa \ln \kappa$). We fix Q , and compare how the choice of N affects the computational complexity. First, let $Q = \Theta(1)$, and compare the results between the two implementations N -loop with $\Theta(\kappa \ln \kappa)$ (Corollary 1) and No-loop with $N = 1$ (Corollary 2). Clearly, the N -loop scheme significantly improves the convergence rate of the No-loop scheme from $\mathcal{O}(\frac{\kappa^6}{K})$ to $\mathcal{O}(\frac{\kappa^4}{K})$, and improves the matrix-vector and gradient complexities from $\tilde{\mathcal{O}}(\kappa^6 \epsilon^{-1})$ and $\tilde{\mathcal{O}}(\kappa^6 \epsilon^{-1})$ to $\tilde{\mathcal{O}}(\kappa^4 \epsilon^{-1})$ and $\tilde{\mathcal{O}}(\kappa^5 \epsilon^{-1})$, respectively. To explain intuitively, the hypergradient estimation involves a coupled error $\eta \|y_k^N - y^*(x_k)\|$ induced from solving the linear system $\nabla_y^2 g(x_k, y_k^N) v = \nabla_y f(x_k, y_k^N)$ with stepsize η . Therefore, a smaller inner-level approximation error $\|y_k^N - y^*(x_k)\|$ allows a more aggressive stepsize η , and hence yields a faster convergence rate as well as a lower total complexity, as also demonstrated in our experiments. It is worth noting that such a comparison is generally different from that in minimax optimization (Lin et al., 2020; Zhang et al., 2020), where alternative (i.e., No-loop) gradient descent ascent (GDA) with $N = 1$ outperforms (N -loop) GDA with $N = \kappa \ln \kappa$, where N denotes the number of ascent iterations for each descent iteration. To explain the reason, in contrast to minimax optimization, the gradient w.r.t. x in bilevel optimization involves **additional** second-order derivatives, which are more sensitive to the inner-level approximation error. Therefore, a larger N is more beneficial for bilevel optimization than minimax optimization. Similarly, we can also fix $Q = \Theta(\kappa \ln \kappa)$, the N - Q -loop scheme with $N = \kappa \ln \kappa$ (Corollary 3) significantly outperforms the Q -loop scheme with $N = 1$ (Corollary 4) in terms of the convergence rate and complexity.

Impact of Q -loop ($Q = 1$ vs $Q = \Theta(\kappa \ln \frac{\kappa}{\epsilon})$). We fix N , and characterize the impact of the choice of Q on the complexity. For $N = 1$, comparing No-loop with $Q = \Theta(1)$ in Corollary 2 and Q -loop with $Q = \Theta(\kappa \ln \kappa)$ in Corollary 4 shows that both choices of Q yield the same matrix-vector complexity $\tilde{\mathcal{O}}(\kappa^6 \epsilon^{-1})$, but Q -loop

with a larger Q improves the gradient complexity of No-loop with $Q = \Theta(1)$ from $\tilde{\mathcal{O}}(\kappa^6 \epsilon^{-1})$ to $\tilde{\mathcal{O}}(\kappa^5 \epsilon^{-1})$. A similar phenomenon can be observed for $N = \Theta(\kappa \ln \kappa)$ based on the comparison between N - Q -loop in Corollary 3 and N -loop in Corollary 1.

In deep learning. Also note that in the setting where the matrix-vector complexity dominates the gradient complexity, e.g., in deep learning, such two choices of Q do not affect the total computational complexity. However, a smaller Q can help reduce the per-iteration load on the computational resource and memory, and hence is preferred in practical applications with large models.

Comparison among four implementations. By comparing the complexity results in Corollaries 1, 2, 3 and 4, it can be seen that N - Q -loop and N -loop (both with a large $N = \Theta(\kappa \ln \kappa)$) achieve the best matrix-vector complexity $\tilde{\mathcal{O}}(\kappa^4 \epsilon^{-1})$, whereas Q -loop and No-loop (both with a smaller $N = 1$) require higher matrix-vector complexity of $\tilde{\mathcal{O}}(\kappa^6 \epsilon^{-1})$. Also note that N - Q -loop has the lowest gradient complexity. This suggests that the introduction of the inner loop with large N can help to reduce the total computational complexity.

5 Convergence Analysis of ITD-BiO

In this section, we first provide a unified theory for ITD-BiO, which is applicable for all choices of N , and then specialize the convergence theory to characterize the computational complexity for the two implementations of ITD-BiO: No loop and N - N -loop. We also provide a convergence lower bound to justify the necessity of choosing large N to achieve a vanishing convergence error. The following theorem characterizes the convergence rate of ITD-BiO for all choices of N .

Theorem 3. *Suppose Assumptions 1, 2, 3 and 4 hold. Define $w = (1 + \frac{2}{\alpha\mu}) \frac{L^2}{\mu^2} (1 - \alpha\mu)^N \lambda_N + \frac{4M^2 w_N^2 L^2}{\mu^2}$ and $\tau = N^2(1 - \alpha\mu)^N + w_N^2 + \lambda_N(1 - \alpha\mu)^N$, where λ_N and w_N are given by $\lambda_N = \frac{4M^2 w_N^2 + 4(1 - \frac{1}{4}\alpha\mu)L^2(1 + \alpha LN)^2}{1 - \frac{1}{4}\alpha\mu - (1 - \alpha\mu)^N(1 + \frac{1}{2}\alpha\mu)}$, $w_N = \alpha \left(\rho + \frac{\alpha \rho L(1 - (1 - \alpha\mu)^{\frac{N}{2}})}{1 - \sqrt{1 - \alpha\mu}} \right) (1 - \alpha\mu)^{\frac{N}{2} - 1} \frac{1 - (1 - \alpha\mu)^{\frac{N}{2}}}{1 - \sqrt{1 - \alpha\mu}}$. Choose parameters such that $\beta^2 \leq \frac{1 - \frac{1}{4}\alpha\mu}{2w}$, $\alpha \leq \frac{1}{2L}$ and $\beta L_\Phi + \frac{8}{\alpha\mu} \left(\frac{1}{2} + \beta L_\Phi \right) w \beta^2 < \frac{1}{4}$, where $L_\Phi = L + \frac{2L^2 + \rho M^2}{\mu} + \frac{2\rho LM + L^3}{\mu^2} + \frac{\rho L^2 M}{\mu^3}$ denotes the smoothness parameter of $\Phi(\cdot)$. Then, we have*

$$\frac{1}{K} \sum_{k=0}^{K-1} \|\nabla \Phi(x_k)\|^2 \leq \mathcal{O} \left(\frac{\Delta_\Phi}{\beta K} + \frac{\tau \Delta_y}{\mu^2 K} + \frac{(1 - \alpha\mu)^{2N}}{\mu^3 K} + \frac{M^2 (1 - \alpha\mu)^{2N} L^2}{\alpha \mu^3} \right), \quad (5)$$

where $\Delta_\Phi = \Phi(x_0) - \min_x \Phi(x)$ and $\Delta_y = \|y_0 - y^*(x_0)\|^2$.

In Theorem 3, the upper bound on the convergence rate for ITD-BiO contains a convergent term $\mathcal{O}(\frac{1}{K})$ (which converges to zero sublinearly with K) and an error term $\mathcal{O}(\frac{M^2(1 - \alpha\mu)^{2N}}{\alpha \mu^3})$ (which is independent of K , and possibly non-vanishing if N is chosen to be small). To show that such a possibly non-vanishing error term (when N is chosen to be small) fundamentally exists, we next provide the following lower bound on the convergence rate of ITD-BiO.

Theorem 4 (Lower Bound). *Consider the ITD-BiO algorithm in Algorithm 2 with $\alpha \leq \frac{1}{L}$, $\beta \leq \frac{1}{L_\Phi}$ and $N \leq \mathcal{O}(1)$, where L_Φ is the smoothness parameter of $\Phi(x)$. There exist objective functions $f(x, y)$ and $g(x, y)$ that satisfy Assumptions 1, 2, 3 and 4 such that for all iterates x_K (where $K \geq 1$) generated by ITD-BiO in Algorithm 2, $\|\nabla \Phi(x_K)\|^2 \geq \Theta(\frac{L^2 M^2}{\mu^2} (1 - \alpha\mu)^{2N})$.*

Clearly, the error term in the upper bound given in Theorem 3 matches the lower bound given in Theorem 4 in terms of $\frac{M^2 L^2}{\mu^2} (1 - \alpha\mu)^{2N}$, and there is still a gap on the order of $\alpha\mu$, which requires future efforts to

address. Theorem 3 and Theorem 4 together indicate that in order to achieve an ϵ -accurate stationary point, N has to be chosen as large as $N = \Theta(\kappa \log \frac{\kappa}{\epsilon})$. This corresponds to the N - N -loop implementation of ITD-BiO, where large N achieves a highly accurate hypergradient estimation in each step. Another No-loop implementation chooses a small constant-level $N = \Theta(1)$ to achieve an efficient execution per step, where a large N can cause large memory usage and computation cost. Following from Theorem 3 and Theorem 4, such No-loop implementation necessarily suffers from a non-vanishing error.

In the following corollaries, we further specialize Theorem 3 to obtain the complexity analysis for ITD-BiO under the two aforementioned implementations of ITD-BiO.

Corollary 5 (N - N -loop). *Consider N - N -loop ITD-BiO with $N = \Theta(\kappa \ln \frac{\kappa}{\epsilon})$. Under the same setting of Theorem 3, choose $\beta = \min \left\{ \sqrt{\frac{\alpha\mu}{40w}}, \sqrt{\frac{1-\frac{\alpha\mu}{4}}{2w}}, \frac{1}{8L_\Phi} \right\}$, $\alpha = \frac{1}{2L}$. Then, $\frac{1}{K} \sum_{k=0}^{K-1} \|\nabla\Phi(x_k)\|^2 = \mathcal{O}(\frac{\kappa^3}{K} + \epsilon)$, and the complexity is $\text{Gc}(\epsilon) = \tilde{\mathcal{O}}(\kappa^4\epsilon^{-1})$, $\text{MV}(\epsilon) = \tilde{\mathcal{O}}(\kappa^4\epsilon^{-1})$.*

Corollary 5 shows that for a large $N = \Theta(\kappa \ln \frac{\kappa}{\epsilon})$, we can guarantee that ITD-BiO converges to an ϵ -accurate stationary point, and the gradient and matrix-vector product complexities are given by $\tilde{\mathcal{O}}(\kappa^4\epsilon^{-1})$. We note that Ji et al. (2021) also analyzed the ITD-BiO with $N = \Theta(\kappa \ln \frac{\kappa}{\epsilon})$, and provided the same complexities as our results in Corollary 5. In comparison, our analysis has several differences. First, Ji et al. (2021) assumed that the minimizer $y^*(x_k)$ at the k^{th} iteration is bounded, whereas our analysis does not impose this assumption. Second, Ji et al. (2021) involved an **additional** error term $\max_{k=1,\dots,K} \|y^*(x_k)\| \frac{L^2 M^2 (1-\alpha\mu)^N}{\mu^4}$, which can be very large (or even unbounded) under standard Assumptions 1, 2, 3 and 4. We next characterize the convergence for the small $N = \Theta(1)$.

Corollary 6 (No-loop). *Consider No-loop ITD-BiO with $N = \Theta(1)$. Under the same setting of Theorem 3, choose stepsizes $\alpha = \frac{1}{2NL}$ and $\beta = \min \left\{ \sqrt{\frac{\alpha\mu}{40w}}, \sqrt{\frac{1-\frac{\alpha\mu}{4}}{2w}}, \frac{1}{8L_\Phi} \right\}$. Then, we have $\frac{1}{K} \sum_{k=0}^{K-1} \|\nabla\Phi(x_k)\|^2 = \mathcal{O}(\frac{\kappa^3}{K} + \frac{M^2 L^2}{\alpha\mu^3})$.*

Corollary 6 indicates that for the constant-level $N = \Theta(1)$, the convergence bound contains a non-vanishing error $\mathcal{O}(\frac{M^2 L^2}{\alpha\mu^3})$. As shown in the convergence lower bound in Theorem 4, under standard Assumptions 1, 2, 3 and 4, such an error is unavoidable. Comparison between the above two corollaries suggests that for ITD-BiO, the N - N -loop is necessary to guarantee a vanishing convergence error, whereas No-loop necessarily suffers from a non-vanishing convergence error.

Discussion on the setting with small response Jacobian. Our results in Theorem 3 and Theorem 4 apply to the general functions whose first- and second-order derivatives are Lipschitz continuous, i.e., under Assumptions 2 and 3. Here, we further discuss the extension of our results to another setting where the response Jacobian is extremely small. This setting occurs in some deep learning applications (Finn et al., 2017; Ji et al., 2020a), where the response Jacobian $\frac{\partial y^*(x)}{\partial x}$ (which is estimated by $\frac{\partial y_k^N(x)}{\partial x}$ with a large N) can be order-of-magnitude smaller than network gradients. Based on eq. (60) and eq. (62) in the appendix, it can be shown that the convergence error is proportional to the quantity $\frac{1}{K} \sum_{k=0}^{K-1} \|\frac{\partial y^*(x_k)}{\partial x_k}\|^2$, and hence the constant-level $N = \Theta(1)$ can still achieve a small error in this setting.

6 Empirical Verification

Experiments on AID-BiO. We first conduct experiments to verify our theoretical results in Corollaries 1, 2, 3 and 4 on AID-BiO with different implementations. We consider the following hyperparameter optimization

problem.

$$\min_{\lambda} \mathcal{L}_{\mathcal{D}_{\text{val}}}(\lambda) = \frac{1}{|\mathcal{D}_{\text{val}}|} \sum_{\xi \in \mathcal{D}_{\text{val}}} \mathcal{L}(w^*; \xi), \quad \text{s.t. } w^* = \arg \min_w \frac{1}{|\mathcal{D}_{\text{tr}}|} \sum_{\xi \in \mathcal{D}_{\text{tr}}} \left(\mathcal{L}(w; \xi) + \frac{\lambda}{2} \|w\|_2^2 \right),$$

where \mathcal{D}_{tr} and \mathcal{D}_{val} stand for training and validation datasets, $\mathcal{L}(w; \xi)$ denotes the loss function induced by the model parameter w and sample ξ , and $\lambda > 0$ denotes the regularization parameter. The goal is to find a good hyperparameter λ to minimize the validation loss evaluated at the optimal model parameters for the regularized empirical risk minimization problem.

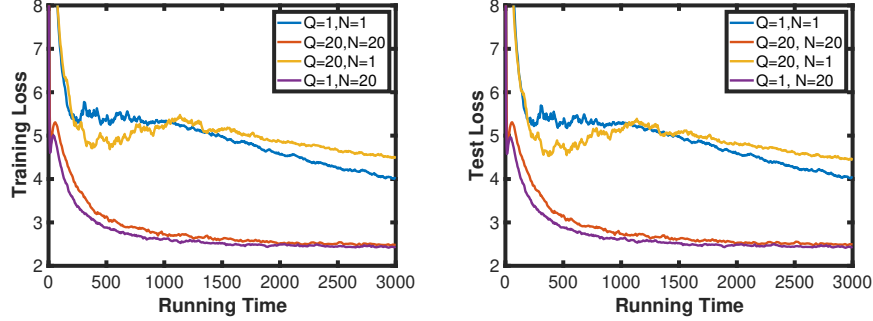


Figure 1: Training and test losses v.s. running time (seconds) on MNIST with different Q and N .

From Figure 1, we can make the following observations. First, the learning curves with $N = 20$ are significantly better than those with $N = 1$, indicating that running multiple steps of gradient descent in the inner loop (i.e., $N > 1$) is crucial for fast convergence. This observation is consistent with our complexity result that N -loop is better than No-loop, and N - Q -loop is better than Q -loop, as shown in Table 1. The reason is that a more accurate hypergradient estimation can accelerate the convergence rate and lead to a reduction on the Jacobian- and Hessian-vector computational complexity. Second, N - Q -loop ($N = 20, Q = 20$) and N -loop ($N = 20, Q = 1$) achieve a comparable convergence performance, and a similar observation can be made for Q -loop ($N = 1, Q = 20$) and No-loop ($N = 1, Q = 1$). This is also consistent with the complexity result provided in Table 1, where different choices of Q do not affect the **dominant** matrix-vector complexity.

Experiments on ITD-BiO. We consider a hyper-representation problem in Sow et al. (2021), where the inner problem is to find optimal regression parameters w and the outer procedure is to find the best representation parameters λ . In specific, the bilevel problem takes the following form:

$$\min_{\lambda} \Phi(\lambda) = \frac{1}{2p} \|h(X_V; \lambda)w^* - Y_V\|^2, \quad \text{s.t. } w^* = \arg \min_w \frac{1}{2q} \|h(X_T; \lambda)w - Y_T\|^2 + \frac{\gamma}{2} \|w\|^2$$

where $X_T \in \mathbb{R}^{q \times m}$ and $X_V \in \mathbb{R}^{p \times m}$ are synthesized training and validation data, $Y_T \in \mathbb{R}^q$, $Y_V \in \mathbb{R}^p$ are their response vectors, and $h(\cdot)$ is a linear transformation. The generation of X_T, X_V, Y_T, Y_V and the experimental setup follow from Sow et al. (2021). We choose $N = 20$ for N - N -loop ITD and $N = 1$ for No-loop ITD. The results are reported with the best-tuned hyperparameters.

Table 3 indicates that N - N -loop with $N = 20$ can achieve a small loss value of 0.004 after 500 total iterations, whereas No-loop with $N = 1$ converges to a much larger loss value of 0.04. This is in consistence with our theoretical results in Table 2, where $N = 1$ can cause a non-vanishing error.

Algorithm	$k = 10$	$k = 50$	$k = 100$	$k = 500$	$k = 1000$
N - N -loop ITD	9.32	0.11	0.01	0.004	0.004
No-loop ITD	435	6.9	0.04	0.04	0.04

Table 3: Validation loss v.s. the number of iterations for ITD-based algorithms.

7 Conclusion

In this paper, we study two popular bilevel optimizers AID-BiO and ITD-BiO, whose implementations potentially involve additional loops of iterations within their base-loop update. By developing unified convergence analysis for all choices of the loop parameters, we are able to provide formal comparison among different implementations. Our result suggests that N -loops are beneficial for better computational efficiency for AID-BiO and for better convergence accuracy for ITD-BiO. This is in contrast to conventional minimax optimization, where No-loop (i.e., single-base-loop) scheme achieves better computational efficiency. Our analysis techniques can be useful to study other bilevel optimizers such as stochastic optimizers and variance reduced optimizers.

References

- Luca Bertinetto, Joao F Henriques, Philip Torr, and Andrea Vedaldi. Meta-learning with differentiable closed-form solvers. In *International Conference on Learning Representations (ICLR)*, 2018.
- Tianyi Chen, Yuejiao Sun, and Wotao Yin. A single-timescale stochastic bilevel optimization method. *arXiv preprint arXiv:2102.04671*, 2021.
- Justin Domke. Generic methods for optimization-based modeling. In *Artificial Intelligence and Statistics (AISTATS)*, pp. 318–326, 2012.
- Matthias Feurer and Frank Hutter. Hyperparameter optimization. In *Automated Machine Learning*, pp. 3–33. Springer, Cham, 2019.
- Chelsea Finn, Pieter Abbeel, and Sergey Levine. Model-agnostic meta-learning for fast adaptation of deep networks. In *Proc. International Conference on Machine Learning (ICML)*, pp. 1126–1135, 2017.
- Rémi Flamary, Alain Rakotomamonjy, and Gilles Gasso. Learning constrained task similarities in graphregularized multi-task learning. *Regularization, Optimization, Kernels, and Support Vector Machines*, pp. 103, 2014.
- Luca Franceschi, Michele Donini, Paolo Frasconi, and Massimiliano Pontil. Forward and reverse gradient-based hyperparameter optimization. In *International Conference on Machine Learning (ICML)*, pp. 1165–1173, 2017.
- Luca Franceschi, Paolo Frasconi, Saverio Salzo, Riccardo Grazi, and Massimiliano Pontil. Bilevel programming for hyperparameter optimization and meta-learning. In *International Conference on Machine Learning (ICML)*, pp. 1568–1577, 2018.
- Saeed Ghadimi and Mengdi Wang. Approximation methods for bilevel programming. *arXiv preprint arXiv:1802.02246*, 2018.

- Riccardo Grazzi, Luca Franceschi, Massimiliano Pontil, and Saverio Salzo. On the iteration complexity of hypergradient computation. In *Proc. International Conference on Machine Learning (ICML)*, 2020.
- Zhishuai Guo and Tianbao Yang. Randomized stochastic variance-reduced methods for stochastic bilevel optimization. *arXiv preprint arXiv:2105.02266*, 2021.
- Zhishuai Guo, Yi Xu, Wotao Yin, Rong Jin, and Tianbao Yang. On stochastic moving-average estimators for non-convex optimization. *arXiv preprint arXiv:2104.14840*, 2021.
- Pierre Hansen, Brigitte Jaumard, and Gilles Savard. New branch-and-bound rules for linear bilevel programming. *SIAM Journal on Scientific and Statistical Computing*, 13(5):1194–1217, 1992.
- Mingyi Hong, Hoi-To Wai, Zhaoran Wang, and Zhuoran Yang. A two-timescale framework for bilevel optimization: Complexity analysis and application to actor-critic. *arXiv preprint arXiv:2007.05170*, 2020.
- Minhui Huang, Kaiyi Ji, Shiqian Ma, and Lifeng Lai. Efficiently escaping saddle points in bilevel optimization. *arXiv preprint arXiv:2202.03684*, 2022.
- Kaiyi Ji and Yingbin Liang. Lower bounds and accelerated algorithms for bilevel optimization. *arXiv preprint arXiv:2102.03926*, 2021.
- Kaiyi Ji, Jason D Lee, Yingbin Liang, and H Vincent Poor. Convergence of meta-learning with task-specific adaptation over partial parameters. *arXiv preprint arXiv:2006.09486*, 2020a.
- Kaiyi Ji, Junjie Yang, and Yingbin Liang. Multi-step model-agnostic meta-learning: Convergence and improved algorithms. *arXiv preprint arXiv:2002.07836*, 2020b.
- Kaiyi Ji, Junjie Yang, and Yingbin Liang. Bilevel optimization: Convergence analysis and enhanced design. In *International Conference on Machine Learning*, pp. 4882–4892. PMLR, 2021.
- Prashant Khanduri, Siliang Zeng, Mingyi Hong, Hoi-To Wai, Zhaoran Wang, and Zhuoran Yang. A near-optimal algorithm for stochastic bilevel optimization via double-momentum. *arXiv preprint arXiv:2102.07367*, 2021.
- Vijay R Konda and John N Tsitsiklis. Actor-critic algorithms. In *Advances in neural information processing systems (NeurIPS)*, pp. 1008–1014, 2000.
- Gautam Kunapuli, Kristin P Bennett, Jing Hu, and Jong-Shi Pang. Classification model selection via bilevel programming. *Optimization Methods & Software*, 23(4):475–489, 2008.
- Yann LeCun, Léon Bottou, Yoshua Bengio, and Patrick Haffner. Gradient-based learning applied to document recognition. *Proceedings of the IEEE*, 86(11):2278–2324, 1998.
- Junyi Li, Bin Gu, and Heng Huang. Improved bilevel model: Fast and optimal algorithm with theoretical guarantee. *arXiv preprint arXiv:2009.00690*, 2020.
- Junyi Li, Bin Gu, and Heng Huang. A fully single loop algorithm for bilevel optimization without hessian inverse. *arXiv preprint arXiv:2112.04660*, 2021.
- Tianyi Lin, Chi Jin, and Michael Jordan. On gradient descent ascent for nonconvex-concave minimax problems. In *International Conference on Machine Learning (ICML)*, pp. 6083–6093. PMLR, 2020.

- Risheng Liu, Pan Mu, Xiaoming Yuan, Shangzhi Zeng, and Jin Zhang. A generic first-order algorithmic framework for bi-level programming beyond lower-level singleton. In *International Conference on Machine Learning (ICML)*, 2020.
- Risheng Liu, Xuan Liu, Xiaoming Yuan, Shangzhi Zeng, and Jin Zhang. A value-function-based interior-point method for non-convex bi-level optimization. In *International Conference on Machine Learning (ICML)*, 2021a.
- Risheng Liu, Yaohua Liu, Shangzhi Zeng, and Jin Zhang. Towards gradient-based bilevel optimization with non-convex followers and beyond. *Advances in Neural Information Processing Systems (NeurIPS)*, 34, 2021b.
- Dougal Maclaurin, David Duvenaud, and Ryan Adams. Gradient-based hyperparameter optimization through reversible learning. In *International Conference on Machine Learning (ICML)*, pp. 2113–2122, 2015.
- Gregory M Moore. *Bilevel programming algorithms for machine learning model selection*. Rensselaer Polytechnic Institute, 2010.
- Fabian Pedregosa. Hyperparameter optimization with approximate gradient. In *International Conference on Machine Learning (ICML)*, pp. 737–746, 2016.
- Aravind Rajeswaran, Chelsea Finn, Sham M Kakade, and Sergey Levine. Meta-learning with implicit gradients. In *Advances in Neural Information Processing Systems (NeurIPS)*, pp. 113–124, 2019.
- Amirreza Shaban, Ching-An Cheng, Nathan Hatch, and Byron Boots. Truncated back-propagation for bilevel optimization. In *International Conference on Artificial Intelligence and Statistics (AISTATS)*, pp. 1723–1732, 2019.
- Chenggen Shi, Jie Lu, and Guangquan Zhang. An extended kuhn–tucker approach for linear bilevel programming. *Applied Mathematics and Computation*, 162(1):51–63, 2005.
- Jake Snell, Kevin Swersky, and Richard Zemel. Prototypical networks for few-shot learning. In *Advances in Neural Information Processing Systems (NIPS)*, 2017.
- Daouda Sow, Kaiyi Ji, and Yingbin Liang. Es-based jacobian enables faster bilevel optimization. *arXiv preprint arXiv:2110.07004*, 2021.
- Daouda Sow, Kaiyi Ji, Ziwei Guan, and Yingbin Liang. A constrained optimization approach to bilevel optimization with multiple inner minima. *arXiv preprint arXiv:2203.01123*, 2022.
- Junjie Yang, Kaiyi Ji, and Yingbin Liang. Provably faster algorithms for bilevel optimization. *Advances in Neural Information Processing Systems (NeurIPS)*, 34, 2021.
- Jiawei Zhang, Peijun Xiao, Ruoyu Sun, and Zhiquan Luo. A single-loop smoothed gradient descent-ascent algorithm for nonconvex-concave min-max problems. *Advances in Neural Information Processing Systems (NeurIPS)*, 33:7377–7389, 2020.

Supplementary Materials

A Expanded Related Work

Gradient-based bilevel optimization. A number of gradient-based bilevel algorithms have been proposed via AID- and ITD-based hypergradient approximations. For example, AID-based hypergradient computation (Domke, 2012; Pedregosa, 2016; Ghadimi & Wang, 2018; Grazi et al., 2020; Ji et al., 2021; Huang et al., 2022) estimates the Hessian-inverse-vector product by solving a linear system with an efficient iterative algorithm. ITD-based hypergradient computation (Maclaurin et al., 2015; Franceschi et al., 2017, 2018; Finn et al., 2017; Shaban et al., 2019; Ji et al., 2020a) involves a backpropagation over the inner-loop gradient-based optimization path. Convergence rate of AID- and ITD-based bilevel methods has been studied recently. For example, Ghadimi & Wang (2018); Ji et al. (2021) and Ji et al. (2021, 2020a) analyzed the convergence rate and complexity of AID- and ITD-based bilevel algorithms, respectively. Ji & Liang (2021) characterized the lower complexity bounds for a class of gradient-based bilevel algorithms. As we mentioned before, previous studies on the convergence rate of deterministic AID-BiO (Ghadimi & Wang, 2018; Ji et al., 2021) focused only on N - Q -loop, and the only convergence rate analysis on ITD-BiO (Ji et al., 2021) was for N - N -loop. Our study here develops unified convergence analysis for all N and Q regimes.

Some works (Liu et al., 2020, 2021a; Li et al., 2020; Sow et al., 2022) studied the convex inner-level objective function with multiple minimizers. Liu et al. (2021b) proposed an initialization auxiliary method for the setting where the inner-level problem is generally nonconvex.

Stochastic bilevel optimization. A variety of stochastic bilevel optimization algorithms have been proposed recently. For example, Ghadimi & Wang (2018); Hong et al. (2020); Ji et al. (2021) proposed stochastic gradient descent (SGD) type of bilevel algorithms, and analyzed their convergence rate and complexity. Some works (Guo & Yang, 2021; Guo et al., 2021; Yang et al., 2021; Khanduri et al., 2021; Chen et al., 2021) then further improved the complexity of SGD type methods using techniques such as variance reduction, momentum acceleration and adaptive learning rate. Sow et al. (2021) proposed a Hessian-free stochastic Evolution Strategies (ES)-based bilevel algorithm with performance guarantee. Although our study mainly focuses on deterministic bilevel optimization, our techniques can be extended to provide refined analysis for stochastic bilevel optimization to capture the order scaling with κ , which is not captured in most of the above studies on stochastic bilevel optimization.

Bilevel optimization for machine learning. Bilevel optimization has shown promise in many machine learning applications such as hyperparameter optimization (Pedregosa, 2016; Franceschi et al., 2018; Ji et al., 2021) and few-shot meta-learning (Finn et al., 2017; Snell et al., 2017; Rajeswaran et al., 2019; Franceschi et al., 2018; Bertinetto et al., 2018; Ji et al., 2020a,b,a). For example, Snell et al. (2017); Bertinetto et al. (2018) introduced an outer-level procedure to learn a common embedding model for all tasks. Ji et al. (2020a) analyzed the convergence rate for meta-learning with task-specific adaptation on partial parameters.

B Further Specifications on Hyperparameter Optimization Experiments

We follow the setting of Yang et al. (2021) to setup the experiment. We first randomly sample 20000 training samples and 10000 test samples from MNIST dataset (LeCun et al., 1998) with 10 classes, and then add a label noise on 10% of the data. The label noise is uniform across all labels from label 0 to label 9. We test algorithms with different values of Q and N to verify our theoretical results. Every algorithm’s learning rates

for inner and outer loops are tuned from the range of $\{0.1, 0.01, 0.001\}$ and we report the result with the best-tuned learning rates. We run 5 random seeds and report the average result. All experiments are run over a single NVIDIA Tesla P100 GPU. The implementations of our experiments are based on the code of Ji et al. (2021), which is under MIT License.

C Proof Sketch of Theorem 1

The proof of Theorem 1 contains three major steps, which include 1) decomposing the hypergradient approximation error into the N -loop error in estimating the inner-level solution and the Q -loop error in solving the linear system approximately, 2) upper-bounding such two types of errors based on the hypergradient approximation errors at previous iterations, and 3) combining all results in the previous steps and proving the convergence guarantee. More detailed steps can be found as below.

Step 1: decomposing hypergradient approximation error.

We first show that the hypergradient approximation error at the k^{th} iteration is bounded by

$$\|\widehat{\nabla}\Phi(x_k) - \nabla\Phi(x_k)\|^2 \leq \underbrace{\left(3L^2 + \frac{3\rho^2 M^2}{\mu^2}\right)\|y_k^* - y_k^N\|^2}_{N\text{-loop estimation error}} + \underbrace{3L^2\|v_k^* - v_k^Q\|^2}_{Q\text{-loop estimation error}}. \quad (6)$$

where the right hand side contains two types of errors induced by solving the inner-level problem and outer-level linear system. Note that for general choices of N and Q , such two errors cannot be guaranteed to be sufficiently small, but fortunately we show via the following results that such errors contain iteratively decreasing components which facilitate the final convergence.

Step 2: upper-bounding linear system approximation error.

We then show that the Q -loop error $\|v_k^* - v_k^Q\|^2$ for solving the linear system is bounded by

$$\begin{aligned} \|v_k^Q - v_k^*\|^2 &\leq \mathcal{O}\left((1 + \eta\mu)(1 - \eta\mu)^{2Q} + w\beta^2\right)\|v_{k-1}^Q - v_{k-1}^*\|^2 \\ &\quad + (\eta^2(1 - \alpha\mu)^N + w\beta^2)\|y_{k-1}^* - y_{k-1}^N\|^2 + w\beta^2\|\nabla\Phi(x_{k-1})\|^2. \end{aligned} \quad (7)$$

Note that if the stepsize β is chosen to be sufficiently small, the right hand side of eq. (7) contains an **iteratively decreasing** term $(1 + \eta\mu)(1 - \eta\mu)^{2Q} + w\beta^2\|v_{k-1}^Q - v_{k-1}^*\|^2$, an error term $(\eta^2(1 - \alpha\mu)^N + w\beta^2)\|y_{k-1}^* - y_{k-1}^N\|^2$ induced by the N -loop updates, and gradient norm term $w\beta^2\|\nabla\Phi(x_{k-1})\|^2$ that captures the increment between two adjacent iterations. Similarly, we upper-bound the N -loop updating error $\|y_k^* - y_k^N\|^2$ by

$$\begin{aligned} \|y_k^N - y_k^*\|^2 &\leq \mathcal{O}\left((1 + \lambda)(1 - \alpha\mu)^N + (1 + \lambda^{-1})\beta^2\right)\|y_{k-1}^N - y_{k-1}^*\|^2 \\ &\quad + (1 + \lambda^{-1})\beta^2\|v_{k-1}^Q - v_{k-1}^*\|^2 + (1 + \lambda^{-1})\beta^2\|\nabla\Phi(x_{k-1})\|^2, \end{aligned} \quad (8)$$

where $\tau = 1 + \frac{1}{\lambda}$ is inversely proportional to λ . Note that we introduce an auxiliary variable λ in the first error term at the right hand side of eq. (8) to allow for a **general choice** of N . To see this, to guarantee that $(1 + \lambda)(1 - \alpha\mu)^N + (1 + \lambda^{-1})\beta^2 < 1$, a larger N allows for a smaller λ . As a result, the outer-level stepsize β can be chosen more aggressively, which hence yields a faster convergence rate but at a cost of N steps of N -loop updates. On the other hand, if N is chosen to be small, e.g., $N = 1$, λ needs to be as small as $\lambda = \Theta(\alpha\mu)$. As a result, β needs to be smaller, and hence yields a slower convergence rate but with a more efficient N -loop update.

Step 3: combining Steps 1 and 2.

Combining eq. (6), eq. (7) and eq. (8), we upper-bound the hypergradient estimation error as

$$\|\widehat{\nabla}\Phi(x_k) - \nabla\Phi(x_k)\|^2 \leq \mathcal{O}((1-\tau)^k + \omega\beta^2 \sum_{j=0}^{k-1} (1-\tau)^j \|\nabla\Phi(x_{k-1-j})\|^2),$$

which, combined with the L_Φ -smoothness property of $\Phi(\cdot)$ and a proper choice of β , yields the final convergence result.

D Proof of Theorem 1

We first provide some auxiliary lemmas to characterize the hypergradient approximation errors.

Lemma 1. *Suppose Assumptions 1, 2, 3 and 4 are satisfied. Let $v_k^* = (\nabla_y^2 g(x_k, y_k^*))^{-1} \nabla_y f(x_k, y_k^*)$ with $y_k^* = \arg \min_y g(x_k, y)$. Then, we have*

$$\begin{aligned} \|v_k^Q - v_k^*\|^2 &\leq (1 + \eta\mu)(1 - \eta\mu)^{2Q} \|v_{k-1}^Q - v_{k-1}^*\|^2 \\ &\quad + 2\left(1 + \frac{1}{\eta\mu}\right) C_Q^2 \|y_k^* - y_k^N\|^2 \\ &\quad + 2(1 - \eta\mu)^{2Q} \left(1 + \frac{1}{\eta\mu}\right) \left(\frac{L}{\mu} + \frac{M\rho}{\mu^2}\right)^2 \left(\frac{L}{\mu} + 1\right)^2 \|x_k - x_{k-1}\|^2, \end{aligned}$$

where $C_Q = \frac{Q(1-\eta\mu)^{Q-1}\rho M\eta}{\mu} + \frac{1-(1-\eta\mu)^Q(1+\eta Q\mu)}{\mu^2} \rho M + (1 - (1 - \eta\mu)^Q) \frac{L}{\mu}$.

Proof. Let v_k^q be the q^{th} ($q = 0, \dots, Q-1$) GD iterate via solving the linear system $\nabla_y^2 g(x_k, y_k^N) v = \nabla_y f(x_k, y_k^N)$, which can be written in the following iterative way.

$$v_k^{q+1} = (I - \eta \nabla_y^2 g(x_k, y_k^N)) v_k^q + \eta \nabla_y f(x_k, y_k^N). \quad (9)$$

Then, by telescoping eq. (9) over q from 0 to Q yields

$$v_k^Q = (I - \eta \nabla_y^2 g(x_k, y_k^N))^Q v_k^0 + \eta \sum_{q=0}^{Q-1} (I - \eta \nabla_y^2 g(x_k, y_k^N))^q \nabla_y f(x_k, y_k^N). \quad (10)$$

Similarly, based on the definition of v_k^* , it can be derived that the following equation holds.

$$v_k^* = (I - \eta \nabla_y^2 g(x_k, y_k^*))^Q v_k^* + \eta \sum_{q=0}^{Q-1} (I - \eta \nabla_y^2 g(x_k, y_k^*))^q \nabla_y f(x_k, y_k^*). \quad (11)$$

Combining eq. (9) and eq. (10), we next characterize the difference between the estimate v_k^Q and the underlying

truth v_k^* . In specific, we have

$$\begin{aligned}
\|v_k^Q - v_k^*\| &\stackrel{(i)}{\leq} \left\| (I - \eta \nabla_y^2 g(x_k, y_k^N))^Q - (I - \eta \nabla_y^2 g(x_k, y_k^*))^Q \right\| \|v_k^*\| + (1 - \eta\mu)^Q \|v_k^0 - v_k^*\| \\
&\quad + \eta \left\| \sum_{q=0}^{Q-1} (I - \eta_y^2 g(x_k, y_k^N))^q - \sum_{q=0}^{Q-1} (I - \eta_y^2 g(x_k, y_k^*))^q \right\| \|\nabla_y f(x_k, y_k^*)\| \\
&\quad + \eta L \left\| \sum_{q=0}^{Q-1} (I - \eta_y^2 g(x_k, y_k^N))^q \right\| \|y_k^* - y_k^N\| \\
&\stackrel{(ii)}{\leq} \left\| (I - \eta \nabla_y^2 g(x_k, y_k^N))^Q - (I - \eta \nabla_y^2 g(x_k, y_k^*))^Q \right\| \frac{M}{\mu} + (1 - \eta\mu)^Q \|v_{k-1}^Q - v_k^*\| \\
&\quad + \eta M \left\| \sum_{q=0}^{Q-1} (I - \eta_y^2 g(x_k, y_k^N))^q - \sum_{q=0}^{Q-1} (I - \eta_y^2 g(x_k, y_k^*))^q \right\| \\
&\quad + (1 - (1 - \eta\mu)^Q) \frac{L}{\mu} \|y_k^* - y_k^N\|. \tag{12}
\end{aligned}$$

where (i) follows from the strong convexity of $g(x, \cdot)$ and (ii) follows from Assumption 4, the warm start initialization $v_k^0 = v_{k-1}^Q$ and $\|v_k^*\| \leq \|(\nabla_y^2 g(x_k, y_k^*))^{-1}\| \|\nabla_y f(x_k, y_k^*)\| \leq \frac{M}{\mu}$. We next provide an upper bound on the quantity $\Delta_q := \|(I - \eta_y^2 g(x_k, y_k^N))^q - (I - \eta_y^2 g(x_k, y_k^*))^q\|$ in eq. (12). In specific, we have

$$\begin{aligned}
\Delta_q &\stackrel{(i)}{\leq} (1 - \eta\mu)\Delta_{q-1} + (1 - \eta\mu)^{q-1} \eta \|\nabla_y^2 g(x_k, y_k^*) - \nabla_y^2 g(x_k, y_k^N)\| \\
&\leq (1 - \eta\mu)\Delta_{q-1} + (1 - \eta\mu)^{q-1} \eta \rho \|y_k^N - y_k^*\|. \tag{13}
\end{aligned}$$

where (i) follows from the strong convexity of $g(x, \cdot)$ and Assumption 3. Telescoping eq. (13) yields

$$\Delta_q \leq (1 - \eta\mu)^q \Delta_0 + q(1 - \eta\mu)^{q-1} \eta \rho \|y_k^N - y_k^*\| = q(1 - \eta\mu)^{q-1} \eta \rho \|y_k^N - y_k^*\|,$$

which, in conjunction with eq. (12), yields

$$\begin{aligned}
\|v_k^Q - v_k^*\| &\leq Q(1 - \eta\mu)^{Q-1} \eta \rho \frac{M}{\mu} \|y_k^N - y_k^*\| + (1 - \eta\mu)^Q \|v_{k-1}^Q - v_k^*\| \\
&\quad + \eta M \sum_{q=0}^{Q-1} q(1 - \eta\mu)^{q-1} \eta \rho \|y_k^N - y_k^*\| + (1 - (1 - \eta\mu)^Q) \frac{L}{\mu} \|y_k^* - y_k^N\|. \tag{14}
\end{aligned}$$

Based on the facts that $\sum_{q=0}^{Q-1} qx^{q-1} = \frac{1-x^Q - Qx^{Q-1} + Qx^Q}{(1-x)^2} > 0$, we obtain from eq. (14) that

$$\begin{aligned}
\|v_k^Q - v_k^*\| &\leq \frac{Q(1 - \eta\mu)^{Q-1} \rho M \eta}{\mu} \|y_k^N - y_k^*\| + (1 - \eta\mu)^Q \|v_{k-1}^Q - v_{k-1}^*\| \\
&\quad + (1 - \eta\mu)^Q \|v_{k-1}^* - v_k^*\| + \frac{1 - (1 - \eta\mu)^Q (1 + \eta Q \mu)}{\mu^2} \rho M \|y_k^N - y_k^*\| \\
&\quad + (1 - (1 - \eta\mu)^Q) \frac{L}{\mu} \|y_k^* - y_k^N\|
\end{aligned}$$

which, in conjunction with $\|v_k^* - v_{k-1}^*\| \leq \left(\frac{L}{\mu} + \frac{M\rho}{\mu^2}\right) \left(\frac{L}{\mu} + 1\right) \|x_k - x_{k-1}\|$ and using the Young's inequality that $\|a + b\|^2 \leq (1 + \eta\mu)\|a\|^2 + (1 + \frac{1}{\eta\mu})\|b\|^2$, completes the proof of Lemma 1. \square

Lemma 2. Suppose Assumptions 1 and 2 are satisfied.

$$\|y_k^* - y_k^N\|^2 \leq (1 - \alpha\mu)^N (1 + \lambda) \|y_{k-1}^N - y_{k-1}^*\|^2 + (1 - \alpha\mu)^N \left(1 + \frac{1}{\lambda}\right) \frac{L^2}{\mu^2} \|x_k - x_{k-1}\|^2 \quad (15)$$

where λ is a positive constant.

Proof. Note that $y_k^* = \arg \min_y g(x_k, y)$. Using the strong convexity (i.e., Assumption 1) and smoothness (i.e., Assumption 2) of $g(x_k, \cdot)$, we have

$$\|y_k^N - y_k^*\|^2 \leq (1 - \alpha\mu)^N \|y_k^0 - y_k^*\|^2, \quad (16)$$

which, in conjunction with the warm start initialization $y_k^0 = y_{k-1}^N$ and using the Young's inequality, yields

$$\begin{aligned} \|y_k^N - y_k^*\|^2 &\leq (1 + \lambda)(1 - \alpha\mu)^N \|y_{k-1}^N - y_{k-1}^*\|^2 + \left(1 + \frac{1}{\lambda}\right)(1 - \alpha\mu)^N \|y_{k-1}^* - y_k^*\|^2 \\ &\stackrel{(i)}{\leq} (1 + \lambda)(1 - \alpha\mu)^N \|y_{k-1}^N - y_{k-1}^*\|^2 + \left(1 + \frac{1}{\lambda}\right)(1 - \alpha\mu)^N \frac{L^2}{\mu^2} \|x_{k-1} - x_k\|^2, \end{aligned} \quad (17)$$

where (i) follows from Lemma 2.2 in Ghadimi & Wang (2018). \square

Lemma 3. Suppose Assumptions 1, 2, 3 and 4 are satisfied. Choose parameters such that $(1 + \lambda)(1 - \alpha\mu)^N (1 + 4r(1 + \frac{1}{\eta\mu})L^2) \leq 1 - \eta\mu$, where the notation $r = \frac{C_Q^2}{(\frac{\rho M}{\mu} + L)^2}$ with C_Q given in Lemma 1. Then, we have the following inequality.

$$\begin{aligned} \|\widehat{\nabla}\Phi(x_k) - \nabla\Phi(x_k)\|^2 &\leq 3L^2(1 - \eta\mu + 6wL^2\beta^2)^k \delta_0 \\ &\quad + 6wL^2\beta^2 \sum_{j=0}^{k-1} (1 - \eta\mu + 6wL^2\beta^2)^j \|\nabla\Phi(x_{k-1-j})\|^2, \end{aligned} \quad (18)$$

where $\delta_0 := (1 + \frac{\rho^2 M^2}{L^2 \mu^2}) \|y_0^N - y_0^*\|^2 + \|v_0^Q - v_0^*\|^2$ and the notation w is given by

$$\begin{aligned} w &= \left(1 + \frac{1}{\lambda}\right)(1 - \alpha\mu)^N \left(1 + \frac{\rho^2 M^2}{L^2 \mu^2}\right) \frac{L^2}{\mu^2} \\ &\quad + 4\left(1 + \frac{1}{\eta\mu}\right) \frac{L^4}{\mu^2} \left(1 + \frac{\rho^2 M^2}{L^2 \mu^2}\right) \left(\frac{4(1 - \eta\mu)^{2Q}}{\mu^2} + r(1 - \alpha\mu)^N \left(1 + \frac{1}{\lambda}\right)\right). \end{aligned} \quad (19)$$

Proof. Combining Lemma 1 and Lemma 2, we have

$$\begin{aligned} \|v_k^Q - v_k^*\|^2 &\leq (1 + \eta\mu)(1 - \eta\mu)^{2Q} \|v_{k-1}^Q - v_{k-1}^*\|^2 \\ &\quad + 2(1 - \alpha\mu)^N (1 + \lambda) \left(1 + \frac{1}{\eta\mu}\right) C_Q^2 \|y_{k-1}^N - y_k^*\|^2 \\ &\quad + 2(1 - \alpha\mu)^N \left(1 + \frac{1}{\lambda}\right) \left(1 + \frac{1}{\eta\mu}\right) C_Q^2 \frac{L^2}{\mu^2} \|x_{k-1} - x_k\|^2 \\ &\quad + 2(1 - \eta\mu)^{2Q} \left(1 + \frac{1}{\eta\mu}\right) \left(\frac{L}{\mu} + \frac{M\rho}{\mu^2}\right)^2 \left(\frac{L}{\mu} + 1\right)^2 \|x_k - x_{k-1}\|^2, \end{aligned}$$

which, in conjunction with $(\frac{L}{\mu} + 1)^2 \leq 4\frac{L^2}{\mu^2}$ and the notation $r = \frac{C_Q^2}{(\frac{\rho M}{\mu} + L)^2}$, yields

$$\begin{aligned} \|v_k^Q - v_k^*\|^2 &\leq (1 + \eta\mu)(1 - \eta\mu)^{2Q} \|v_{k-1}^Q - v_{k-1}^*\|^2 \\ &\quad + 2\left(1 + \frac{1}{\eta\mu}\right) \frac{L^2}{\mu^2} \left(\frac{L}{\mu} + \frac{\rho M}{\mu}\right)^2 \left(\frac{4(1 - \eta\mu)^{2Q}}{\mu^2} + r(1 - \alpha\mu)^N \left(1 + \frac{1}{\lambda}\right)\right) \|x_k - x_{k-1}\|^2 \\ &\quad + 2(1 + \lambda)(1 - \alpha\mu)^N \left(1 + \frac{1}{\eta\mu}\right) \left(\frac{\rho M}{\mu} + L\right)^2 r \|y_{k-1}^N - y_{k-1}^*\|^2. \end{aligned} \quad (20)$$

Then, combining Lemma 2 and eq. (20), we have

$$\begin{aligned}
& \left(1 + \frac{\rho^2 M^2}{L^2 \mu^2}\right) \|y_k^N - y_k^*\|^2 + \|v_k^Q - v_k^*\|^2 \\
& \leq (1 + \lambda)(1 - \alpha\mu)^N \left(1 + \frac{\rho^2 M^2}{L^2 \mu^2}\right) \|y_{k-1}^N - y_{k-1}^*\|^2 \\
& \quad + \left(1 + \frac{1}{\lambda}\right)(1 - \alpha\mu)^N \left(1 + \frac{\rho^2 M^2}{L^2 \mu^2}\right) \frac{L^2}{\mu^2} \|x_{k-1} - x_k\|^2 \\
& \quad + (1 + \eta\mu)(1 - \eta\mu)^{2Q} \|v_{k-1}^Q - v_{k-1}^*\|^2 \\
& \quad + 4\left(1 + \frac{1}{\eta\mu}\right)(1 + \lambda)\left(L^2 + \frac{\rho^2 M^2}{\mu^2}\right)(1 - \alpha\mu)^N r \|y_{k-1}^N - y_{k-1}^*\|^2 \\
& \quad + 4\left(1 + \frac{1}{\eta\mu}\right) \frac{L^4}{\mu^2} \left(1 + \frac{\rho^2 M^2}{\mu^2 L^2}\right) \left(\frac{4(1 - \eta\mu)^{2Q}}{\mu^2} + r(1 - \alpha\mu)^N \left(1 + \frac{1}{\lambda}\right)\right) \|x_{k-1} - x_k\|^2
\end{aligned}$$

which, in conjunction with the definition of w in eq. (19), yields

$$\begin{aligned}
& \left(1 + \frac{\rho^2 M^2}{L^2 \mu^2}\right) \|y_k^N - y_k^*\|^2 + \|v_k^Q - v_k^*\|^2 \\
& \leq (1 + \lambda)(1 - \alpha\mu)^N \left(1 + \frac{\rho^2 M^2}{L^2 \mu^2}\right) \left(1 + 4r\left(1 + \frac{1}{\eta\mu}\right)L^2\right) \|y_{k-1}^N - y_{k-1}^*\|^2 \\
& \quad + (1 + \eta\mu)(1 - \eta\mu)^{2Q} \|v_{k-1}^Q - v_{k-1}^*\|^2 + w \|x_{k-1} - x_k\|^2.
\end{aligned} \tag{21}$$

For notational convenience, we define $\delta_k := \left(1 + \frac{\rho^2 M^2}{L^2 \mu^2}\right) \|y_k^N - y_k^*\|^2 + \|v_k^Q - v_k^*\|^2$ as the per-iteration error induced by y_k^N and v_k^Q . Then, recalling that $(1 + \lambda)(1 - \alpha\mu)^N (1 + 4r(1 + \frac{1}{\eta\mu})L^2) \leq 1 - \eta\mu$, we obtain from eq. (21) that

$$\delta_k \leq (1 - \eta\mu)\delta_{k-1} + 2w\beta^2 \|\nabla\Phi(x_{k-1}) - \widehat{\nabla}\Phi(x_{k-1})\|^2 + 2w\beta^2 \|\nabla\Phi(x_{k-1})\|^2. \tag{22}$$

Based on the form of $\widehat{\nabla}\Phi(x_k)$ and $\nabla\Phi(x_k)$ in eq. (3) and eq. (2), we have

$$\begin{aligned}
\|\widehat{\nabla}\Phi(x_k) - \nabla\Phi(x_k)\|^2 & \leq 3\|\nabla_x f(x_k, y_k^*) - \nabla_x f(x_k, y_k^N)\|^2 + 3\|\nabla_x \nabla_y g(x_k, y_k^N)\|^2 \|v_k^* - v_k^Q\|^2 \\
& \quad + 3\|\nabla_x \nabla_y g(x_k, y_k^*) - \nabla_x \nabla_y g(x_k, y_k^N)\|^2 \|v_k^*\|^2,
\end{aligned}$$

which, in conjunction with Assumptions 1, 2, 3 and 4, yields

$$\|\widehat{\nabla}\Phi(x_k) - \nabla\Phi(x_k)\|^2 \leq \left(3L^2 + \frac{3\rho^2 M^2}{\mu^2}\right) \|y_k^* - y_k^N\|^2 + 3L^2 \|v_k^* - v_k^Q\|^2. \tag{23}$$

Substituting eq. (23) into eq. (22) yields

$$\delta_k \leq (1 - \eta\mu + 6wL^2\beta^2)\delta_{k-1} + 2w\beta^2 \|\nabla\Phi(x_{k-1})\|^2,$$

which, by telescoping and using eq. (23), finishes the proof. \square

Proof of Theorem 1

First, based on Lemma 2 in Ji et al. (2021), we have $\nabla\Phi(\cdot)$ is L_Φ -Lipschitz, where $L_\Phi = L + \frac{2L^2 + \rho M^2}{\mu} + \frac{2\rho LM + L^3}{\mu^2} + \frac{\rho L^2 M}{\mu^3} = \Theta(\kappa^3)$. Then, we have

$$\begin{aligned}\Phi(x_{k+1}) &\leq \Phi(x_k) + \langle \nabla\Phi(x_k), x_{k+1} - x_k \rangle + \frac{L_\Phi}{2} \|x_{k+1} - x_k\|^2 \\ &\leq \Phi(x_k) - \left(\frac{\beta}{2} - \beta^2 L_\Phi\right) \|\nabla\Phi(x_k)\|^2 + \left(\frac{\beta}{2} + \beta^2 L_\Phi\right) \|\nabla\Phi(x_k) - \widehat{\nabla}\Phi(x_k)\|^2 \\ &\stackrel{(i)}{\leq} \Phi(x_k) - \left(\frac{\beta}{2} - \beta^2 L_\Phi\right) \|\nabla\Phi(x_k)\|^2 + \left(\frac{\beta}{2} + \beta^2 L_\Phi\right) 3L^2\delta_0(1 - \eta\mu + 6wL^2\beta^2)^k \\ &\quad + 6wL^2\beta^2 \left(\frac{\beta}{2} + \beta^2 L_\Phi\right) \sum_{j=0}^{k-1} (1 - \eta\mu + 6wL^2\beta^2)^j \|\nabla\Phi(x_{k-1-j})\|^2,\end{aligned}\tag{24}$$

where (i) follows from Lemma 3, δ_0 is defined in Lemma 3 and w is given by eq. (19). Then, telescoping eq. (24) over k from 0 to $K-1$, denoting $x^* = \arg\min_x \Phi(x)$ and using, we have

$$\begin{aligned}&\left(\frac{\beta}{2} - \beta^2 L_\Phi\right) \sum_{k=0}^{K-1} \|\nabla\Phi(x_k)\|^2 \\ &\leq \Phi(x_0) - \Phi(x^*) + \frac{3L^2\delta_0(\frac{\beta}{2} + \beta^2 L_\Phi)}{\eta\mu - 6wL^2\beta^2} \\ &\quad + 6wL^2\beta^2 \left(\frac{\beta}{2} + \beta^2 L_\Phi\right) \sum_{k=0}^{K-1} \sum_{j=0}^{k-1} (1 - \eta\mu + 6wL^2\beta^2)^j \|\nabla\Phi(x_{k-1-j})\|^2 \\ &\stackrel{(i)}{\leq} \Phi(x_0) - \Phi(x^*) + \frac{3L^2\delta_0(\frac{\beta}{2} + \beta^2 L_\Phi)}{\eta\mu - 6wL^2\beta^2} + 6wL^2\beta^2 \left(\frac{\beta}{2} + \beta^2 L_\Phi\right) \frac{\sum_{j=0}^{K-1} \|\nabla\Phi(x_j)\|^2}{\eta\mu - 6wL^2\beta^2}\end{aligned}\tag{25}$$

where (i) follows because $\sum_{k=0}^{K-1} \sum_{j=0}^{k-1} a_j b_{k-1-j} \leq \sum_{k=0}^{K-1} a_k \sum_{j=0}^{K-1} b_j$. Rearranging eq. (25) yields

$$\begin{aligned}&\left(\frac{1}{2} - \beta L_\Phi - \frac{6wL^2\beta^2(\frac{1}{2} + \beta L_\Phi)}{\eta\mu - 6wL^2\beta^2}\right) \frac{1}{K} \sum_{k=0}^{K-1} \|\nabla\Phi(x_k)\|^2 \\ &\leq \frac{\Phi(x_0) - \Phi(x^*)}{\beta K} + \frac{3L^2\delta_0(\frac{1}{2} + \beta L_\Phi)}{\eta\mu - 6wL^2\beta^2} \frac{1}{K}.\end{aligned}\tag{26}$$

Note that $(1 + \lambda)(1 - \alpha\mu)^N(1 + 4r(1 + \frac{1}{\eta\mu})L^2) \leq 1 - \eta\mu$ and $r > 1$, we have

$$3\eta^2(1 - \alpha\mu)^N \left(1 + \frac{1}{\lambda}\right) \leq \frac{1 - \eta\mu}{1 + \lambda} \frac{3\eta^2(1 + \frac{1}{\lambda})}{1 + 4r(1 + \frac{1}{\eta\mu})L^2} \leq \frac{1 - \eta\mu}{\lambda} \frac{\eta^3\mu}{rL^2},\tag{27}$$

which, combined with the definitions of w and \tilde{w} given by eq. (19) and theorem 1, yields $w \leq \tilde{w}$. Then, since we set $6\tilde{w}L^2\beta^2 \leq \frac{\eta\mu}{3}$ in Theorem 1, we have $\frac{6wL^2\beta^2}{\eta\mu - 6wL^2\beta^2} < \frac{6\tilde{w}L^2\beta^2}{\eta\mu - 6\tilde{w}L^2\beta^2} < \frac{1}{2}$, which, combined with eq. (26), yields

$$\left(\frac{1}{4} - \frac{3}{2}\beta L_\Phi\right) \frac{1}{K} \sum_{k=0}^{K-1} \|\nabla\Phi(x_k)\|^2 \leq \frac{\Phi(x_0) - \Phi(x^*)}{\beta K} + \frac{9L^2\delta_0(\frac{1}{2} + \beta L_\Phi)}{2\eta\mu K},$$

which, in conjunction with $\beta \leq \frac{1}{12L_\Phi}$, yields

$$\frac{1}{K} \sum_{k=0}^{K-1} \|\nabla\Phi(x_k)\|^2 \leq \frac{8(\Phi(x_0) - \Phi(x^*))}{\beta K} + \frac{21L^2\delta_0}{\eta\mu K}.\tag{28}$$

Based on the updates of y and v , we have

$$\begin{aligned} \|y_0^N - y_0^*\|^2 &\leq \|y_0^0 - y_0^*\|^2 = \|y_0^*\|^2 \\ \|v_0^Q - v_0^*\| &\leq \|v_0^*\| + \|v_0^Q - (\nabla_y^2 g(x_0, y_0^N))^{-1} \nabla_y f(x_0, y_0^N)\| + \|(\nabla_y^2 g(x_0, y_0^N))^{-1} \nabla_y f(x_0, y_0^N)\| \\ &\stackrel{(i)}{\leq} \frac{M}{\mu} + \frac{2}{\mu} (L\|y_0^*\| + M), \end{aligned} \quad (29)$$

where (i) follows because the initialization $v_0^0 = 0$ and $y_0^0 = 0$. Substituting eq. (29) into $\delta_0 := (1 + \frac{\rho^2 M^2}{L^2 \mu^2}) \|y_0^N - y_0^*\|^2 + \|v_0^Q - v_0^*\|^2$ and eq. (28), we complete the proof.

E Proof of Corollary 1

In this case, first note that all choices of η, α, λ and N satisfy the conditions in Theorem 1. First recall that $r = \frac{C_Q^2}{(\frac{\rho M}{\mu} + L)^2}$, where

$$C_Q = \frac{Q(1 - \eta\mu)^{Q-1} \rho M \eta}{\mu} + \frac{1 - (1 - \eta\mu)^Q (1 + \eta Q \mu)}{\mu^2} \rho M + (1 - (1 - \eta\mu)^Q) \frac{L}{\mu},$$

which, combined with $Q = \Theta(1)$ and $\eta = \Theta(1)$, yields $C_Q^2 = \Theta(\kappa^2)$ and hence $r = \Theta(1)$. Note that $\tilde{w} := \frac{(1-\eta\mu)\eta\mu}{3\lambda r L^2} (1 + \frac{\rho^2 M^2}{L^2 \mu^2}) \frac{L^2}{\mu^2} + (1 + \frac{1}{\eta\mu}) (L^2 + \frac{\rho^2 M^2}{\mu^2}) (\frac{16(1-\eta\mu)^{2Q}}{\mu^2} + \frac{4(1-\eta\mu)\eta\mu}{3\lambda L^2}) \frac{L^2}{\mu^2}$, which, combined with $\eta = \frac{1}{L}$ and $\lambda = 1$, yields $\tilde{w} = \Theta(\kappa^3 + \kappa^7) = \Theta(\kappa^7)$. Based on the choice of β , we have

$$\beta = \min \left\{ \frac{1}{12L_\Phi}, \sqrt{\frac{\eta\mu}{18L^2\tilde{w}}} \right\} = \Theta(\kappa^{-4}).$$

Then, we have the following convergence result.

$$\frac{1}{K} \sum_{k=0}^{K-1} \|\nabla \Phi(x_k)\|^2 = \mathcal{O}\left(\frac{\kappa^4}{K} + \frac{\kappa^3}{K}\right).$$

Then, to achieve an ϵ -accurate stationary point, we have $K = \mathcal{O}(\kappa^4 \epsilon^{-1})$, and hence we have the following complexity results.

- Gradient complexity: $\text{Gc}(\epsilon) = K(N + 2) = \tilde{\mathcal{O}}(\kappa^5 \epsilon^{-1})$.
- Matrix-vector product complexities:

$$\text{MV}(\epsilon) = K + KQ = \tilde{\mathcal{O}}(\kappa^4 \epsilon^{-1}).$$

Then, the proof is complete.

F Proof of Corollary 2

Based on the choices of α, λ and $\eta \leq \frac{1}{\mu Q}$, recalling $r = \frac{C_Q^2}{(\frac{\rho M}{\mu} + L)^2}$ and using the inequality that $(1-x)^Q \geq 1-Qx$ for any $0 < x < 1$, we have

$$r \leq \frac{(\frac{\rho M \eta Q}{\mu} + \eta^2 Q^2 \rho M + \eta Q L)^2}{(\frac{\rho M}{\mu} + L)^2} \leq 4\eta^2 Q^2,$$

which, in conjunction with $\eta \leq \frac{1}{128} \frac{\alpha \mu^2}{Q^2 L^2}$, yields

$$\begin{aligned} (1 + \lambda)(1 - \alpha\mu)^N (1 + 4r(1 + \frac{1}{\eta\mu})L^2) &\leq (1 + \lambda)(1 - \alpha\mu)^N (1 + 16(1 + \frac{1}{\eta\mu})\eta^2 Q^2 L^2) \\ &\leq 1 - \frac{\alpha\mu}{4} \leq 1 - \eta\mu, \end{aligned}$$

and hence all requirements in Theorem 1 are satisfied. Also, similarly to the proof of Corollary 1, we have $r = \Theta(1)$, which, combined with $\eta = \Theta(\kappa^{-2})$, yields $\tilde{w} = \Theta(\kappa^6 + \kappa^9) = \Theta(\kappa^9)$, and hence

$$\beta = \min \left\{ \frac{1}{12L_\Phi}, \sqrt{\frac{\eta\mu}{18L^2\tilde{w}}} \right\} = \Theta(\kappa^{-6}).$$

Then, we have the following convergence result.

$$\frac{1}{K} \sum_{k=0}^{K-1} \|\nabla\Phi(x_k)\|^2 = \mathcal{O}\left(\frac{\kappa^6}{K} + \frac{\kappa^5}{K}\right).$$

Then, to achieve an ϵ -accurate stationary point, we have $K = \mathcal{O}(\kappa^6 \epsilon^{-1})$, and hence we have the following complexity results.

- Gradient complexity: $\text{Gc}(\epsilon) = 3K = \tilde{\mathcal{O}}(\kappa^6 \epsilon^{-1})$.
- Matrix-vector product complexities:

$$\text{MV}(\epsilon) = K + KQ = \tilde{\mathcal{O}}(\kappa^6 \epsilon^{-1}).$$

Then, the proof is complete.

G Proof of Theorem 2

Using an approach similar to eq. (14) in Lemma 1, we have

$$\|v_k^Q - v_k^*\|^2 \leq 2C_Q^2 \|y_k^* - y_k^N\|^2 + 2(1 - \eta\mu)^{2Q} \|v_k^0 - v_k^*\|^2, \quad (30)$$

where C_Q is defined in Lemma 1. Using the zero initialization v_k^0 and based on the fact that $\|v_k^*\| \leq \frac{M}{\mu}$, we obtain from eq. (30) that

$$\|v_k^Q - v_k^*\|^2 \leq 2C_Q^2 \|y_k^* - y_k^N\|^2 + \frac{2(1 - \eta\mu)^{2Q} M^2}{\mu^2},$$

which, in conjunction with eq. (23), yields

$$\|\widehat{\nabla}\Phi(x_k) - \nabla\Phi(x_k)\|^2 \leq \left(3L^2 + \frac{3\rho^2 M^2}{\mu^2} + 6L^2 C_Q^2\right) \|y_k^N - y_k^*\|^2 + \frac{6L^2(1 - \eta\mu)^{2Q} M^2}{\mu^2}. \quad (31)$$

Then, substituting eq. (31) into Lemma 2, and using the definition of τ in Theorem 2, we have

$$\begin{aligned} \|y_k^* - y_k^N\|^2 &\leq (1 - \alpha\mu)^N (1 + \lambda) \|y_{k-1}^N - y_{k-1}^*\|^2 + 2(1 - \alpha\mu)^N \left(1 + \frac{1}{\lambda}\right) \frac{L^2}{\mu^2} \beta^2 \|\nabla\Phi(x_{k-1})\|^2 \\ &\quad + 2(1 - \alpha\mu)^N \left(1 + \frac{1}{\lambda}\right) \frac{L^2}{\mu^2} \beta^2 \|\widehat{\nabla}\Phi(x_{k-1}) - \nabla\Phi(x_{k-1})\|^2 \\ &\leq \tau \|y_{k-1}^N - y_{k-1}^*\|^2 + 2(1 - \alpha\mu)^N \left(1 + \frac{1}{\lambda}\right) \frac{L^2}{\mu^2} \beta^2 \|\nabla\Phi(x_{k-1})\|^2 \\ &\quad + 12(1 - \alpha\mu)^N \left(1 + \frac{1}{\lambda}\right) \frac{L^4 M^2}{\mu^4} \beta^2 (1 - \eta\mu)^{2Q}. \end{aligned} \quad (32)$$

Telescoping eq. (32) over k yields

$$\begin{aligned} \|y_k^* - y_k^N\|^2 &\leq \tau^k \|y_0^* - y_0^N\|^2 + 2(1 - \alpha\mu)^N \left(1 + \frac{1}{\lambda}\right) \frac{L^2}{\mu^2} \beta^2 \sum_{j=0}^{k-1} \tau^j \|\nabla\Phi(x_{k-1-j})\|^2 \\ &\quad + \frac{12}{1 - \tau} (1 - \alpha\mu)^N \left(1 + \frac{1}{\lambda}\right) \frac{L^4 M^2}{\mu^4} \beta^2 (1 - \eta\mu)^{2Q}, \end{aligned}$$

which, in conjunction with eq. (31), $\|y_0^* - y_0^N\|^2 \leq (1 - \alpha\mu)^N \|y_0 - y_0^*\|^2$, the notation of w in Theorem 2 and $\delta_0 = 3(L^2 + \frac{\rho^2 M^2}{\mu^2} + 2L^2 C_Q^2)(1 - \alpha\mu)^N \|y_0^* - y_0\|^2$, yields

$$\begin{aligned} \|\widehat{\nabla}\Phi(x_k) - \nabla\Phi(x_k)\|^2 &\leq \delta_0 \tau^k + 6L^2(1 - \eta\mu)^{2Q} \frac{M^2}{\mu^2} + w\beta^2 \sum_{j=0}^{k-1} \tau^j \|\nabla\Phi(x_{k-1-j})\|^2 \\ &\quad + \frac{6wL^2 M^2}{(1 - \tau)\mu^2} (1 - \eta\mu)^{2Q} \beta^2. \end{aligned} \tag{33}$$

Then, using an approach similar to eq. (24), we have

$$\begin{aligned} \Phi(x_{k+1}) &\leq \Phi(x_k) - \left(\frac{\beta}{2} - \beta^2 L_\Phi\right) \|\nabla\Phi(x_k)\|^2 + \left(\frac{\beta}{2} + \beta^2 L_\Phi\right) \|\nabla\Phi(x_k) - \widehat{\nabla}\Phi(x_k)\|^2 \\ &\stackrel{(i)}{\leq} \Phi(x_k) - \left(\frac{\beta}{2} - \beta^2 L_\Phi\right) \|\nabla\Phi(x_k)\|^2 + \left(\frac{\beta}{2} + \beta^2 L_\Phi\right) \delta_0 \tau^k \\ &\quad + w\beta^2 \left(\frac{\beta}{2} + \beta^2 L_\Phi\right) \sum_{j=0}^{k-1} \tau^j \|\nabla\Phi(x_{k-1-j})\|^2 + \frac{6L^2 M^2}{\mu^2} \left(\frac{\beta}{2} + \beta^2 L_\Phi\right) (1 - \eta\mu)^{2Q} \\ &\quad + \left(\frac{\beta}{2} + \beta^2 L_\Phi\right) \frac{6wL^2 M^2}{(1 - \tau)\mu^2} (1 - \eta\mu)^{2Q} \beta^2, \end{aligned} \tag{34}$$

where (i) follows from eq. (33). Then, rearranging the above eq. (34), we have

$$\begin{aligned} &\frac{1}{K} \left(\frac{1}{2} - \beta L_\Phi\right) \sum_{k=0}^{K-1} \|\nabla\Phi(x_k)\|^2 \\ &\leq \frac{\Phi(x_0) - \Phi(x^*)}{\beta K} + \frac{1}{K} \left(\frac{1}{2} + \beta L_\Phi\right) \frac{\delta_0}{1 - \tau} \\ &\quad + w\beta^2 \left(\frac{1}{2} + \beta L_\Phi\right) \frac{1}{K} \sum_{k=0}^{K-1} \sum_{j=0}^{k-1} \tau^j \|\nabla\Phi(x_{k-1-j})\|^2 + \frac{6L^2 M^2}{\mu^2} \left(\frac{1}{2} + \beta L_\Phi\right) (1 - \eta\mu)^{2Q} \\ &\quad + \left(\frac{1}{2} + \beta L_\Phi\right) \frac{6wL^2 M^2}{(1 - \tau)\mu^2} (1 - \eta\mu)^{2Q} \beta^2, \end{aligned}$$

which, in conjunction with the inequality that $\sum_{k=0}^{K-1} \sum_{j=0}^{k-1} a_j b_{k-1-j} \leq \sum_{k=0}^{K-1} a_k \sum_{j=0}^{K-1} b_j$, yields

$$\begin{aligned} &\left(\frac{1}{2} - \beta L_\Phi - w\beta^2 \left(\frac{1}{2} + \beta L_\Phi\right) \frac{1}{1 - \tau}\right) \frac{1}{K} \sum_{k=0}^{K-1} \|\nabla\Phi(x_k)\|^2 \\ &\leq \frac{\Phi(x_0) - \Phi(x^*)}{\beta K} + \frac{1}{K} \left(\frac{1}{2} + \beta L_\Phi\right) \frac{\delta_0}{1 - \tau} + \frac{6L^2 M^2}{\mu^2} \left(\frac{1}{2} + \beta L_\Phi\right) (1 - \eta\mu)^{2Q} \\ &\quad + \left(\frac{1}{2} + \beta L_\Phi\right) \frac{6wL^2 M^2}{(1 - \tau)\mu^2} (1 - \eta\mu)^{2Q} \beta^2. \end{aligned} \tag{35}$$

Using $\beta L_\Phi + w\beta^2\left(\frac{1}{2} + \beta L_\Phi\right)\frac{1}{1-\tau} \leq \frac{1}{4}$ in the above eq. (35) yields

$$\frac{1}{K} \sum_{k=0}^{K-1} \|\nabla \Phi(x_k)\|^2 \leq \frac{4(\Phi(x_0) - \Phi(x^*))}{\beta K} + \frac{3}{K} \frac{\delta_0}{1-\tau} + \frac{27L^2M^2}{\mu^2}(1-\eta\mu)^{2Q},$$

which finishes the proof.

H Proof of Corollary 3

Note that we choose $N = c_n \kappa \ln \frac{\kappa}{\epsilon}$ and $Q = c_q \kappa \ln \frac{\kappa}{\epsilon}$. Then, for proper constants c_n and c_q , we have $\beta L_\Phi < \frac{1}{8}$, $C_Q = \Theta(\kappa^2)$, $\tau = \Theta(1)$ and $w\beta^2\left(\frac{1}{2} + \beta L_\Phi\right)\frac{1}{1-\tau} < \frac{1}{8}$. Then, we have

$$\frac{1}{K} \sum_{k=0}^{K-1} \|\nabla \Phi(x_k)\|^2 = \mathcal{O}\left(\frac{\kappa^3}{K} + \epsilon\right).$$

To achieve an ϵ -accurate stationary point, the complexity is given by

- Gradient complexity: $\text{Gc}(\epsilon) = K(N+2) = \tilde{\mathcal{O}}(\kappa^4 \epsilon^{-1})$.
- Matrix-vector product complexities: $\text{MV}(\epsilon) = K + KQ = \tilde{\mathcal{O}}(\kappa^4 \epsilon^{-1})$.

The proof is then complete.

I Proof of Corollary 4

Choose $Q = c_q \kappa \ln \frac{\kappa}{\epsilon}$. Then, for a proper selection of the constant c_q , we have $C_Q = \Theta(\kappa^2)$. To guarantee $6\left(1 + \frac{1}{\lambda}\right)\frac{L^2}{\mu^2}(L^2 + \frac{\rho^2 M^2}{\mu^2} + 2L^2 C_Q^2)\beta^2 \leq \frac{\alpha\mu}{4}$, we choose $\beta = \Theta(\kappa^{-4})$, which implies $1 - \tau = \Theta(\alpha\mu)$. In addition, we have $w = \Theta(\kappa^7)$ and hence $\delta_0/(1-\tau) = \mathcal{O}(\kappa^5)$. Then, we have

$$\frac{1}{K} \sum_{k=0}^{K-1} \|\nabla \Phi(x_k)\|^2 = \mathcal{O}\left(\frac{\kappa^5}{K} + \frac{\kappa^4}{K} + \epsilon\right).$$

Then, to achieve an ϵ -accurate stationary point, the complexity is given by

- Gradient complexity: $\text{Gc}(\epsilon) = K(N+2) = \tilde{\mathcal{O}}(\kappa^5 \epsilon^{-1})$.
- Matrix-vector product complexities: $\text{MV}(\epsilon) = K + KQ = \tilde{\mathcal{O}}(\kappa^6 \epsilon^{-1})$.

Then, the proof is complete.

J Proof of Theorem 3

We first provide two useful lemmas, which are then used to prove Theorem 3.

Lemma 4. *Suppose Assumptions 1, 2 and 3 are satisfied. Choose inner stepsize $\alpha < \frac{1}{L}$. Then, we have*

$$\left\| \frac{\partial y_k^N}{\partial x_k} - \frac{\partial y^*(x_k)}{\partial x_k} \right\| \leq (1 - \alpha\mu)^N \left\| \frac{\partial y^*(x_k)}{\partial x_k} \right\| + w_N \|y_k^0 - y^*(x_k)\|,$$

where we define

$$w_N = \alpha \left(\rho + \frac{\alpha \rho L (1 - (1 - \alpha\mu)^{\frac{N}{2}})}{1 - \sqrt{1 - \alpha\mu}} \right) (1 - \alpha\mu)^{\frac{N}{2} - 1} \frac{1 - (1 - \alpha\mu)^{\frac{N}{2}}}{1 - \sqrt{1 - \alpha\mu}}. \quad (36)$$

Proof. Based on the updates of ITD-based method in Algorithm 2, we have, for $j = 1, \dots, N$,

$$\frac{\partial y_k^j}{\partial x_k} = \frac{\partial y_k^{j-1}}{\partial x_k} - \alpha \nabla_x \nabla_y g(x_k, y_k^{j-1}) - \alpha \frac{\partial y_k^{j-1}}{\partial x_k} \nabla_y^2 g(x_k, y_k^{j-1}),$$

which, in conjunction with the fact that $\frac{\partial y_k^0}{\partial x_k} = 0$, yields

$$\frac{\partial y_k^N}{\partial x_k} = -\alpha \sum_{j=0}^{N-1} \nabla_x \nabla_y g(x_k, y_k^j) \prod_{i=j+1}^{N-1} (I - \alpha \nabla_y^2 g(x_k, y_k^i)). \quad (37)$$

Then, based on the optimality condition of $y^*(x)$ and using the chain rule, we have

$$\nabla_x \nabla_y g(x_k, y^*(x_k)) + \frac{\partial y^*(x_k)}{\partial x_k} \nabla_y^2 g(x_k, y^*(x_k)) = 0,$$

which further yields

$$\begin{aligned} \frac{\partial y^*(x_k)}{\partial x_k} &= \frac{\partial y^*(x_k)}{\partial x_k} \prod_{j=0}^{N-1} (I - \alpha \nabla_y^2 g(x_k, y^*(x_k))) \\ &\quad - \alpha \sum_{j=0}^{N-1} \nabla_x \nabla_y g(x_k, y^*(x_k)) \prod_{i=j+1}^{N-1} (I - \alpha \nabla_y^2 g(x_k, y^*(x_k))). \end{aligned} \quad (38)$$

For the case where $N = 1$, based on eq. (37) and eq. (38), we have

$$\left\| \frac{\partial y_k^N}{\partial x_k} - \frac{\partial y^*(x_k)}{\partial x_k} \right\| \leq (1 - \alpha\mu) \left\| \frac{\partial y^*(x_k)}{\partial x_k} \right\| + \alpha\rho \|y_k^0 - y^*(x_k)\|. \quad (39)$$

Next, we prove the case where $N \geq 2$. By subtracting eq. (37) by eq. (38), we have

$$\begin{aligned} \left\| \frac{\partial y_k^N}{\partial x_k} - \frac{\partial y^*(x_k)}{\partial x_k} \right\| &\leq (1 - \alpha\mu)^N \left\| \frac{\partial y^*(x_k)}{\partial x_k} \right\| \\ &\quad + \alpha \sum_{j=0}^{N-1} \underbrace{\left\| \nabla_x \nabla_y g(x_k, y_k^j) \prod_{i=j+1}^{N-1} (I - \alpha \nabla_y^2 g(x_k, y_k^i)) - \nabla_x \nabla_y g(x_k, y^*(x_k)) \prod_{i=j+1}^{N-1} (I - \alpha \nabla_y^2 g(x_k, y^*(x_k))) \right\|}_{\Delta_j}, \end{aligned} \quad (40)$$

where we define Δ_j for notational convenience. Note that Δ_j is upper-bounded by

$$\begin{aligned} \Delta_j &\leq (1 - \alpha\mu)^{N-1-j} \rho \|y_k^j - y^*(x_k)\| \\ &\quad + L \underbrace{\left\| \prod_{i=j+1}^{N-1} (I - \alpha \nabla_y^2 g(x_k, y_k^i)) - \prod_{i=j+1}^{N-1} (I - \alpha \nabla_y^2 g(x_k, y^*(x_k))) \right\|}_{M_{j+1}}. \end{aligned} \quad (41)$$

For notational simplicity, we define a quantity M_{j+1} in eq. (41) for the case where the product index starts from $j+1$. Next we upper-bound M_{j+1} via the following steps.

$$\begin{aligned} M_{j+1} &\leq (1 - \alpha\mu) M_{j+2} + (1 - \alpha\mu)^{N-j-2} \alpha\rho \|y_k^{j+1} - y^*(x_k)\| \\ &\stackrel{(i)}{\leq} (1 - \alpha\mu) M_{j+2} + (1 - \alpha\mu)^{N-j-2} \alpha\rho (1 - \alpha\mu)^{\frac{j+1}{2}} \|y_k^0 - y^*(x_k)\| \\ &\leq (1 - \alpha\mu) M_{j+2} + (1 - \alpha\mu)^{N-\frac{j}{2}-\frac{3}{2}} \alpha\rho \|y_k^0 - y^*(x_k)\|, \end{aligned} \quad (42)$$

where (i) follows by applying gradient descent to the strongly-convex smooth function $g(x_k, \cdot)$. Telescoping eq. (42) further yields

$$\begin{aligned}
M_{j+1} &\leq (1-\alpha\mu)^{N-j-2}M_{N-1} + \sum_{i=j+2}^{N-1} (1-\alpha\mu)^{i-j-2}(1-\alpha\mu)^{N-\frac{i-2}{2}-\frac{3}{2}}\alpha\rho\|y_k^0 - y^*(x_k)\| \\
&\leq (1-\alpha\mu)^{N-j-2}M_{N-1} + \sum_{i=0}^{N-j-3} (1-\alpha\mu)^i(1-\alpha\mu)^{N-\frac{j}{2}-\frac{i}{2}-\frac{3}{2}}\alpha\rho\|y_k^0 - y^*(x_k)\| \\
&\leq (1-\alpha\mu)^{N-j-2}\alpha\rho(1-\alpha\mu)^{\frac{N-1}{2}}\|y_k^0 - y^*(x_k)\| \\
&\quad + \sum_{i=0}^{N-j-3} (1-\alpha\mu)^{N-\frac{j}{2}+\frac{i}{2}-\frac{3}{2}}\alpha\rho\|y_k^0 - y^*(x_k)\| \\
&\leq \sum_{i=0}^{N-j-2} (1-\alpha\mu)^{N-\frac{j}{2}+\frac{i}{2}-\frac{3}{2}}\alpha\rho\|y_k^0 - y^*(x_k)\|,
\end{aligned}$$

which, in conjunction with $\sum_{i=0}^{N-j-2}(1-\alpha\mu)^{\frac{i}{2}} \leq \frac{1-(1-\alpha\mu)^{\frac{N}{2}}}{1-\sqrt{1-\alpha\mu}}$, yields

$$M_{j+1} \leq \frac{\alpha\rho(1-(1-\alpha\mu)^{\frac{N}{2}})}{1-\sqrt{1-\alpha\mu}}(1-\alpha\mu)^{N-\frac{j}{2}-\frac{3}{2}}\|y_k^0 - y^*(x_k)\|. \quad (43)$$

Then, substituting eq. (43) into eq. (41) yields

$$\begin{aligned}
\Delta_j &\leq (1-\alpha\mu)^{N-1-\frac{j}{2}}\rho\|y_k^0 - y^*(x_k)\| \\
&\quad + \frac{\alpha\rho L(1-(1-\alpha\mu)^{\frac{N}{2}})}{1-\sqrt{1-\alpha\mu}}(1-\alpha\mu)^{N-\frac{3}{2}-\frac{j}{2}}\|y_k^0 - y^*(x_k)\|.
\end{aligned} \quad (44)$$

Summing up eq. (44) over j from 0 to $N-1$ yields

$$\sum_{j=0}^{N-1} \Delta_j \leq \left(\rho + \frac{\alpha\rho L(1-(1-\alpha\mu)^{\frac{N}{2}})}{1-\sqrt{1-\alpha\mu}}\right)\|y_k^0 - y^*(x_k)\|(1-\alpha\mu)^{\frac{N}{2}-1}\frac{1-(1-\alpha\mu)^{\frac{N}{2}}}{1-\sqrt{1-\alpha\mu}}. \quad (45)$$

Then, substituting eq. (45) into eq. (40) and using the notation w_N in eq. (36), we have

$$\left\|\frac{\partial y_k^N}{\partial x_k} - \frac{\partial y^*(x_k)}{\partial x_k}\right\| \leq (1-\alpha\mu)^N \left\|\frac{\partial y^*(x_k)}{\partial x_k}\right\| + w_N\|y_k^0 - y^*(x_k)\|. \quad (46)$$

Combining eq. (39) (i.e., $N=1$ case) and eq. (46) (i.e., $N \geq 2$ case) completes the proof. \square

Lemma 5. Suppose Assumptions 1, 2, 3 and 4 hold. Define

$$\lambda_N = \frac{4M^2w_N^2 + 4(1-\frac{1}{4}\alpha\mu)L^2(1+\alpha LN)^2}{1-\frac{1}{4}\alpha\mu - (1-\alpha\mu)^N(1+\frac{1}{2}\alpha\mu)}$$

and $w = (1+\frac{2}{\alpha\mu})\frac{L^2}{\mu^2}(1-\alpha\mu)^N\lambda_N + \frac{4M^2w_N^2L^2}{\mu^2}$, where w_N is given in eq. (36). Let $\delta_k = \|\widehat{\nabla}\Phi(x_k) - \nabla\Phi(x_k)\|^2 + (\lambda_N - 4L^2(1+\alpha LN)^2)\|y_k^N - y^*(x_k)\|^2$ denote the approximation error at the k^{th} iteration. Choose stepsizes $\beta^2 \leq \frac{1-\frac{1}{4}\alpha\mu}{2w}$ and $\alpha \leq \frac{1}{2L}$. Then, we have

$$\delta_k \leq \left(1 - \frac{1}{4}\alpha\mu\right)^k \delta_0 + J_k(1-\alpha\mu)^{2N} + 2w\beta^2 \sum_{j=0}^{k-1} \left(1 - \frac{1}{4}\alpha\mu\right)^{k-1-j} \|\nabla\Phi(x_j)\|^2,$$

where $J_k = \sum_{j=0}^{k-1} \left(1 - \frac{1}{4}\alpha\mu\right)^j 4M^2 \left\|\frac{\partial y^*(x_{k-j})}{\partial x_{k-j}}\right\|^2$ is related to Jacobian matrix of response function.

Proof. First note that using the chain rule, $\widehat{\nabla}\Phi(x_k)$ and $\nabla\Phi(x_k)$ can be written as

$$\begin{aligned}\widehat{\nabla}\Phi(x_k) &= \nabla_x f(x_k, y_k^N) + \frac{\partial y_k^N}{\partial x_k} \nabla_y f(x_k, y_k^N), \\ \nabla\Phi(x_k) &= \nabla_x f(x_k, y^*(x_k)) + \frac{\partial y^*(x_k)}{\partial x_k} \nabla_y f(x_k, y^*(x_k)).\end{aligned}\tag{47}$$

Subtracting two equations in eq. (47), we have

$$\begin{aligned}\|\widehat{\nabla}\Phi(x_k) - \nabla\Phi(x_k)\| &\leq L\|y_k^N - y^*(x_k)\| \\ &\quad + \left\| \frac{\partial y_k^N}{\partial x_k} \right\| L\|y_k^N - y^*(x_k)\| + M \left\| \frac{\partial y^*(x_k)}{\partial x_k} - \frac{\partial y_k^N}{\partial x_k} \right\|,\end{aligned}\tag{48}$$

which, in conjunction with $\left\| \frac{\partial y_k^N}{\partial x_k} \right\| = \|\alpha \sum_{j=0}^{N-1} \nabla_x \nabla_y g(x_k, y_k^j) \prod_{i=j+1}^{N-1} (I - \alpha \nabla_y^2 g(x_k, y_k^i))\| \leq \alpha L \sum_{j=0}^{N-1} (1 - \alpha\mu)^{N-1-j} \leq \alpha L N$, yields

$$\begin{aligned}\|\widehat{\nabla}\Phi(x_k) - \nabla\Phi(x_k)\| &\leq L(1 + \alpha L N) \|y_k^N - y^*(x_k)\| + M \left\| \frac{\partial y^*(x_k)}{\partial x_k} - \frac{\partial y_k^N}{\partial x_k} \right\| \\ &\stackrel{(i)}{\leq} (L + \alpha L^2 N) \|y_k^N - y^*(x_k)\| + M \left\| \frac{\partial y^*(x_k)}{\partial x_k} \right\| (1 - \alpha\mu)^N \\ &\quad + M w_N \|y_k^0 - y^*(x_k)\|,\end{aligned}\tag{49}$$

where (i) follows from Lemma 4. Using $\|y_k^0 - y^*(x_k)\| = \|y_{k-1}^N - y^*(x_k)\| \leq \|y_{k-1}^N - y^*(x_{k-1})\| + \frac{L}{\mu} \|x_k - x_{k-1}\|$ and taking the square on both sides of eq. (49), we have

$$\begin{aligned}\|\widehat{\nabla}\Phi(x_k) - \nabla\Phi(x_k)\|^2 &\leq 4L^2(1 + \alpha L N)^2 \|y_k^N - y^*(x_k)\|^2 + 4M^2 \left\| \frac{\partial y^*(x_k)}{\partial x_k} \right\|^2 (1 - \alpha\mu)^{2N} \\ &\quad + 4M^2 w_N^2 \|y_{k-1}^N - y^*(x_{k-1})\|^2 + 4M^2 w_N^2 \frac{L^2}{\mu^2} \|x_k - x_{k-1}\|^2.\end{aligned}\tag{50}$$

In the meanwhile, based on Lemma 2, we have,

$$\begin{aligned}\|y_k^N - y^*(x_k)\|^2 &\leq (1 - \alpha\mu)^N \left(1 + \frac{1}{2}\alpha\mu\right) \|y_{k-1}^N - y^*(x_{k-1})\|^2 \\ &\quad + \left(1 + \frac{2}{\alpha\mu}\right) \frac{L^2}{\mu^2} (1 - \alpha\mu)^N \|x_{k-1} - x_k\|^2.\end{aligned}\tag{51}$$

Based on $\alpha \leq \frac{1}{2L}$ and the form of λ_N in Lemma 5, we have $\lambda_N > 4L^2(1 + \alpha L N)^2 > 0$. Then, multiplying eq. (51) by λ_N and adding eq. (50), we have

$$\begin{aligned}\|\widehat{\nabla}\Phi(x_k) - \nabla\Phi(x_k)\|^2 &+ \left(\lambda_N - 4L^2(1 + \alpha L N)^2\right) \|y_k^N - y^*(x_k)\|^2 \\ &\leq \left(1 - \frac{1}{4}\alpha\mu\right) \left(\lambda_N - 4L^2(1 + \alpha L N)^2\right) \|y_{k-1}^N - y^*(x_{k-1})\|^2 + 4M^2 \left\| \frac{\partial y^*(x_k)}{\partial x_k} \right\|^2 (1 - \alpha\mu)^{2N} \\ &\quad + \left(\left(1 + \frac{2}{\alpha\mu}\right) \frac{L^2}{\mu^2} (1 - \alpha\mu)^N \lambda_N + 4M^2 w_N^2 \frac{L^2}{\mu^2}\right) \|x_k - x_{k-1}\|^2,\end{aligned}\tag{52}$$

which, in conjunction with $\|x_k - x_{k-1}\|^2 = \beta^2 \|\widehat{\nabla}\Phi(x_{k-1})\|^2 \leq 2\beta^2 \|\widehat{\nabla}\Phi(x_{k-1}) - \nabla\Phi(x_{k-1})\|^2 + 2\beta^2 \|\nabla\Phi(x_{k-1})\|^2$ and using the notation of w in Lemma 5, yields

$$\begin{aligned}\|\widehat{\nabla}\Phi(x_k) - \nabla\Phi(x_k)\|^2 &+ \left(\lambda_N - 4L^2(1 + \alpha L N)^2\right) \|y_k^N - y^*(x_k)\|^2 \\ &\leq \left(1 - \frac{1}{4}\alpha\mu\right) \left(\lambda_N - 4L^2(1 + \alpha L N)^2\right) \|y_{k-1}^N - y^*(x_{k-1})\|^2 + 4M^2 \left\| \frac{\partial y^*(x_k)}{\partial x_k} \right\|^2 (1 - \alpha\mu)^{2N} \\ &\quad + 2\beta^2 w \|\widehat{\nabla}\Phi(x_{k-1}) - \nabla\Phi(x_{k-1})\|^2 + 2\beta^2 w \|\nabla\Phi(x_{k-1})\|^2.\end{aligned}\tag{53}$$

Using $\beta^2 \leq \frac{1-\frac{1}{4}\alpha\mu}{2w}$ and the notation $\delta_k = \|\widehat{\nabla}\Phi(x_k) - \nabla\Phi(x_k)\|^2 + (\lambda_N - 4L^2(1 + \alpha LN)^2)\|y_k^N - y^*(x_k)\|^2$ in the above eq. (53) yields

$$\delta_k \leq 4M^2 \left\| \frac{\partial y^*(x_k)}{\partial x_k} \right\|^2 (1 - \alpha\mu)^{2N} + \left(1 - \frac{1}{4}\alpha\mu\right) \delta_{k-1} + 2w\beta^2 \|\nabla\Phi(x_{k-1})\|^2. \quad (54)$$

Telescoping the above eq. (54) over k yields

$$\begin{aligned} \delta_k &\leq \left(1 - \frac{1}{4}\alpha\mu\right)^k \delta_0 + \sum_{j=0}^{k-1} \left(1 - \frac{1}{4}\alpha\mu\right)^j 4M^2 \left\| \frac{\partial y^*(x_{k-j})}{\partial x_{k-j}} \right\|^2 (1 - \alpha\mu)^{2N} \\ &\quad + 2w\beta^2 \sum_{j=0}^{k-1} \left(1 - \frac{1}{4}\alpha\mu\right)^{k-1-j} \|\nabla\Phi(x_j)\|^2, \end{aligned}$$

which, in conjunction with the definition of J_k , finishes the proof. \square

Proof of Theorem 3

Choose the same stepsizes α and β as in Lemma 5. Then, based on the smoothness of $\Phi(\cdot)$ (i.e., Lemma 2 in Ji et al. (2021)), we have

$$\begin{aligned} \Phi(x_{k+1}) &\leq \Phi(x_k) - \left(\frac{\beta}{2} - \beta^2 L_\Phi\right) \|\nabla\Phi(x_k)\|^2 + \left(\frac{\beta}{2} + \beta^2 L_\Phi\right) \|\nabla\Phi(x_k) - \widehat{\nabla}\Phi(x_k)\|^2 \\ &\stackrel{(i)}{\leq} \Phi(x_k) - \left(\frac{\beta}{2} - \beta^2 L_\Phi\right) \|\nabla\Phi(x_k)\|^2 + \left(\frac{\beta}{2} + \beta^2 L_\Phi\right) \delta_0 \left(1 - \frac{1}{4}\alpha\mu\right)^k \\ &\quad + 2\left(\frac{\beta}{2} + \beta^2 L_\Phi\right) w\beta^2 \sum_{j=0}^{k-1} \left(1 - \frac{1}{4}\alpha\mu\right)^{k-1-j} \|\nabla\Phi(x_j)\|^2 \\ &\quad + \left(\frac{\beta}{2} + \beta^2 L_\Phi\right) J_k (1 - \alpha\mu)^{2N} \end{aligned} \quad (55)$$

where (i) follows from Lemma 5 with $\delta_k \geq \|\widehat{\nabla}\Phi(x_k) - \nabla\Phi(x_k)\|^2$. Then, telescoping the above eq. (55) over k from 0 to $K-1$ yields

$$\begin{aligned} \left(\frac{\beta}{2} - \beta^2 L_\Phi\right) \sum_{k=0}^{K-1} \|\nabla\Phi(x_k)\|^2 &\leq \Phi(x_0) - \Phi(x^*) + \frac{4\beta(\frac{1}{2} + \beta L_\Phi) \delta_0}{\alpha\mu} \\ &\quad + \sum_{k=0}^{K-1} J_k \beta \left(\frac{1}{2} + \beta L_\Phi\right) (1 - \alpha\mu)^{2N} \\ &\quad + 2\left(\frac{\beta}{2} + \beta^2 L_\Phi\right) w\beta^2 \sum_{k=0}^{K-1} \sum_{j=0}^{k-1} \left(1 - \frac{1}{4}\alpha\mu\right)^{k-1-j} \|\nabla\Phi(x_j)\|^2, \end{aligned} \quad (56)$$

which, combined with $\sum_{k=0}^{K-1} \sum_{j=0}^{k-1} (1 - \frac{1}{4}\alpha\mu)^{k-1-j} \|\nabla\Phi(x_j)\|^2 \leq \frac{4}{\alpha\mu} \sum_{j=0}^{K-1} \|\nabla\Phi(x_j)\|^2$, yields

$$\begin{aligned} &\left(\frac{1}{2} - \beta L_\Phi - \frac{8}{\alpha\mu} \left(\frac{1}{2} + \beta L_\Phi\right) w\beta^2\right) \frac{1}{K} \sum_{k=0}^{K-1} \|\nabla\Phi(x_k)\|^2 \\ &\leq \frac{\Phi(x_0) - \Phi(x^*)}{\beta K} + \frac{4(\frac{1}{2} + \beta L_\Phi) \delta_0}{\alpha\mu K} + \left(\frac{1}{2} + \beta L_\Phi\right) (1 - \alpha\mu)^{2N} \frac{1}{K} \sum_{k=0}^{K-1} J_k. \end{aligned} \quad (57)$$

Based on the definition of J_k in Lemma 5, we have

$$\sum_{k=0}^{K-1} J_k = \sum_{k=0}^{K-1} \sum_{j=0}^{k-1} \left(1 - \frac{1}{4}\alpha\mu\right)^j 4M^2 \left\| \frac{\partial y^*(x_{k-j})}{\partial x_{k-j}} \right\|^2 \stackrel{(i)}{\leq} \frac{16M^2}{\alpha\mu} \sum_{k=0}^{K-1} \left\| \frac{\partial y^*(x_k)}{\partial x_k} \right\|^2, \quad (58)$$

where (i) follows from the inequality that $\sum_{k=0}^{K-1} \sum_{j=0}^{k-1} a_j b_{k-1-j} \leq \sum_{k=0}^{K-1} a_k \sum_{j=0}^{K-1} b_j$. Choose β such that $\beta L_\Phi + \frac{8}{\alpha\mu} \left(\frac{1}{2} + \beta L_\Phi\right) w \beta^2 < \frac{1}{4}$. In addition, based on eq. (49), recalling the definition that $\delta_0 = \|\hat{\nabla}\Phi(x_0) - \nabla\Phi(x_0)\|^2 + (\lambda_N - 4L^2(1 + \alpha LN)^2) \|y_0^N - y^*(x_0)\|^2$, using the fact that $\|\frac{\partial y^*(x_0)}{\partial x_0}\| \leq \frac{L}{\mu}$, we have

$$\delta_0 \leq \mathcal{O}\left((N^2(1 - \alpha\mu)^N + w_N^2 + \lambda_N(1 - \alpha\mu)^N) \|y_0 - y^*(x_0)\|^2 + \frac{L^2 M^2}{\mu^2} (1 - \alpha\mu)^{2N}\right). \quad (59)$$

Recall the definition $\tau = N^2(1 - \alpha\mu)^N + w_N^2 + \lambda_N(1 - \alpha\mu)^N$. Then, substituting eq. (58) and eq. (59) into eq. (57) yields

$$\begin{aligned} \frac{1}{K} \sum_{k=0}^{K-1} \|\nabla\Phi(x_k)\|^2 &\leq \mathcal{O}\left(\frac{\Phi(x_0) - \Phi(x^*)}{\beta K} + \frac{\tau \|y_0 - y^*(x_0)\|^2}{\mu^2 K} + \frac{(1 - \alpha\mu)^{2N}}{\mu^3 K} \right. \\ &\quad \left. + \frac{M^2}{\alpha\mu} (1 - \alpha\mu)^{2N} \frac{1}{K} \sum_{k=0}^{K-1} \left\| \frac{\partial y^*(x_k)}{\partial x_k} \right\|^2\right), \end{aligned} \quad (60)$$

which, in conjunction with $\|\frac{\partial y^*(x)}{\partial x}\| \leq \frac{L}{\mu}$, completes the proof.

K Proof of Corollary 5

Based on the choice of α and N and using $\epsilon < 1$, we have $w = \Theta(\sqrt{\epsilon}\kappa^2)$

$$\tau = \frac{(\ln \frac{\kappa}{\epsilon})^2}{\kappa^2} \sqrt{\epsilon} + \sqrt{\epsilon} + \frac{\epsilon + \sqrt{\epsilon}\kappa^2(\ln \frac{\kappa}{\epsilon})^2}{\kappa^4} = \mathcal{O}(1), \quad (61)$$

which, in conjunction with $\beta = \min\left\{\sqrt{\frac{\alpha\mu}{40w}}, \sqrt{\frac{1 - \frac{\alpha\mu}{4}}{2w}}, \frac{1}{8L_\Phi}\right\}$, yields $\beta = \Theta(\kappa^{-3})$. Substituting eq. (61) and $\beta = \Theta(\kappa^{-3})$ into eq. (5) yields

$$\frac{1}{K} \sum_{k=0}^{K-1} \|\nabla\Phi(x_k)\|^2 = \mathcal{O}\left(\frac{\kappa^3}{K} + \epsilon\right).$$

Then, to achieve an ϵ -accurate stationary point, we have $K = \mathcal{O}(\kappa^3 \epsilon^{-1})$, and hence we have the following complexity results.

- Gradient complexity: $\text{Gc}(\epsilon) = K(N + 2) = \mathcal{O}(\kappa^4 \epsilon^{-1} \ln \frac{\kappa}{\epsilon})$.
- Matrix-vector product complexities:

$$\text{MV}(\epsilon) = 2KN = \mathcal{O}(\kappa^4 \epsilon^{-1} \ln \frac{\kappa}{\epsilon}).$$

Then, the proof is complete.

L Proof of Corollary 6

Based on the choice of α and N , we have

$$\begin{aligned} w_N &= \Theta(\alpha(\rho + \alpha\rho LN)N) = \Theta(1), \\ \lambda_N &= \frac{4M^2w_N^2 + 4(1 - \frac{1}{4}\alpha\mu)L^2(1 + \alpha LN)^2}{1 - \frac{1}{4}\alpha\mu - (1 - \alpha\mu)^N(1 + \frac{1}{2}\alpha\mu)} = \Theta(\kappa), \end{aligned}$$

and hence $w = \Theta(\kappa^4)$ and $\tau = \Theta(\kappa)$. Then, we have $\beta = \Theta(\kappa^3)$, and hence we obtain from eq. (5) that

$$\frac{1}{K} \sum_{k=0}^{K-1} \|\nabla\Phi(x_k)\|^2 = \mathcal{O}\left(\frac{\kappa^3}{K} + \frac{M^2L^2}{\alpha\mu^3}\right),$$

which finishes the proof.

M Proof of Theorem 4

We consider the following construction of loss functions.

$$\begin{aligned} f(x, y) &= \frac{1}{2}x^T Z_x x + M\mathbf{1}^T y \\ g(x, y) &= \frac{1}{2}y^T Z_y y - Lx^T y + \mathbf{1}^T y, \end{aligned} \tag{62}$$

where $Z_x = Z_y = \begin{bmatrix} L & 0 \\ 0 & \mu \end{bmatrix}$ and M is a positive constant. First note that the minimizer of inner-level function $g(x, \cdot)$ and the total gradient $\nabla\Phi(x)$ are given by

$$\begin{aligned} y^*(x) &= Z_y^{-1}(Lx - \mathbf{1}), \\ \nabla\Phi(x) &= Z_x x + LMZ_y^{-1}\mathbf{1}. \end{aligned} \tag{63}$$

Based on the updates of ITD-based method in Algorithm 2, we have, for $t = 0, \dots, N$

$$y_k^t = y_k^{t-1} - \alpha(Z_y y_k^{t-1} - Lx_k + \mathbf{1}). \tag{64}$$

Taking the derivative w.r.t. x_k on the both sides of eq. (64) yields

$$\frac{\partial y_k^t}{\partial x_k} = (I - \alpha Z_y) \frac{\partial y_k^{t-1}}{\partial x_k} + \alpha L I, \tag{65}$$

Telescoping the above eq. (65) over t from 1 to N and using the fact that $\frac{\partial y_k^0}{\partial x_k} = 0$, yields

$$\frac{\partial y_k^N}{\partial x_k} = \alpha L \sum_{t=0}^{N-1} (I - \alpha Z_y)^t,$$

which, in conjunction with the update $x_{k+1} = x_k - \beta \frac{\partial f(x_k, y_k^N)}{\partial x_k}$, yields

$$x_{k+1} = x_k - \beta \left(Z_x x_k + \alpha L M \sum_{t=0}^{N-1} (I - \alpha Z_y)^t \mathbf{1} \right). \tag{66}$$

For notational convenience, let $Z_N = \alpha \sum_{t=0}^{N-1} (I - \alpha Z_y)^t$ and $x_0 = \mathbf{1}$. Telescoping eq. (66) over k from 0 to $K - 1$ yields

$$\begin{aligned}
x_K &= (I - \beta Z_x)^K \mathbf{1} - LM \sum_{k=0}^{K-1} (I - \beta Z_x)^k \beta Z_N \mathbf{1} \\
&= (I - \beta Z_x)^K \mathbf{1} - LM Z_x^{-1} Z_N \mathbf{1} + LM \sum_{k=K}^{\infty} (I - \beta Z_x)^k \beta Z_N \mathbf{1} \\
&= (I - \beta Z_x)^K \mathbf{1} - LM Z_x^{-1} Z_N \mathbf{1} + LM (I - \beta Z_x)^K Z_x^{-1} Z_N \mathbf{1}.
\end{aligned} \tag{67}$$

Rearranging the above eq. (67) yields

$$\begin{aligned}
&\|Z_x(x_K + LM Z_x^{-1} Z_N \mathbf{1})\|^2 \\
&= \|Z_x(I - \beta Z_x)^K \mathbf{1} + LM(I - \alpha Z_y)^N Z_y^{-1} \mathbf{1} + LM(I - \beta Z_x)^K Z_N \mathbf{1}\|^2 \\
&\geq L^2 M^2 \|(I - \alpha Z_y)^N Z_y^{-1} \mathbf{1}\|^2 + \|Z_x(I - \beta Z_x)^K \mathbf{1}\|^2 + L^2 M^2 \|(I - \beta Z_x)^K Z_N \mathbf{1}\|^2
\end{aligned}$$

which, in conjunction with $\alpha \leq \frac{1}{L}$, yields

$$\|\nabla \Phi(x_K)\|^2 \geq L^2 M^2 \|(I - \alpha Z_y)^N Z_y^{-1} \mathbf{1}\|^2 = \Theta\left(\frac{L^2 M^2}{\mu^2} (1 - \alpha \mu)^{2N}\right), \tag{68}$$

which holds for all K .